

Wing Sail Performance Compared to a Traditional Sail on Sailing Craft

A project present to
The Faculty of the Department of Aerospace Engineering
San Jose State University

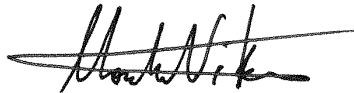
in partial fulfillment of the requirements for the degree
Master of Science in Aerospace Engineering

By

Harrison Turner

May 2015

approved by



Dr. Nikos Mourtos

Faculty Advisor



Abstract

In the history of sailing, specifically the America's Cup, the development of new technologies and methods for making a boat go faster have led to leaps in the field that have resonated throughout the industry and beyond. One such innovation was that of a wing sail in place of the traditional fabric sail. The recent America's Cup matches have shown that at high wind speeds and in large applications, the wing sail is much more efficient and capable of producing higher boat speeds than that of a traditional sail. It is worth investigating whether or not these principles hold true for small sailboats at relatively low wind speeds. In this paper, it is shown through theoretical modeling using Computational Fluid Dynamics (CFD) as well as a practical experimentation using a small sailboat that the wing sail performs at least similar and most of the time better than the traditional sail for the given parameters. The results of this paper prove that the application of wing sails can be used for smaller boats as well as larger boats as was previously known. These results also show that for any use of sailing methodologies, a wing sail can be used instead of a traditional sail for greater performance.

Acknowledgements

I would like to thank San Jose State University and its faculty, administrators and board for giving me the opportunity to study and earn a degree. I would specifically like to thank Dr. Mourtos for giving me the inspiration and guidance for this project.

I would also like to thank my family, starting with my parents, Ann and Rick. They pushed me (especially my mother) to further my education beyond my Bachelor's Degree while being fully employed in order to become a more well-rounded engineer with a brighter future. I would also like to thank my wife, Cindy, for continuing to push me to finish this degree after taking a leave of absence to start our family. Without her willpower, I do not know if I would have been able to complete this degree. I would also like to thank my son, Pierce. You light up my life each and every day and are my true inspiration.

I likewise owe thanks to Kristopher Hoard and Kelsey Gram who helped me with my testing by recording data and observations during the testing.

Contents

| | |
|---|----|
| List of Figures..... | v |
| List of Tables..... | vi |
| List of Nomenclature..... | vi |
| 1. Introduction..... | 1 |
| 1.1. History of the America’s Cup and Wing Sails..... | 1 |
| 1.2. Other Uses of Wing Sails in Sailing Endeavors..... | 4 |
| 1.3. Motivation for Project..... | 5 |
| 2. Forces Acting on a Sailboat and its Sail..... | 6 |
| 3. Theoretical Analysis of Traditional Sails and Wing Sails..... | 10 |
| 3.1. Computational Fluid Dynamics Theory..... | 10 |
| 3.2. Theoretical Experiment Setup..... | 12 |
| 3.3. Results of Theoretical Experiment..... | 13 |
| 3.4. Discussion of Theoretical Experimental Analysis..... | 17 |
| 4. Practical Experimental Analysis of Traditional Sails and Wing Sails..... | 18 |
| 4.1. Practical Experimental Setup..... | 18 |
| 4.2. Results of Practical Experiment..... | 23 |
| 4.3. Discussion of Practical Experimental Analysis..... | 25 |
| 5. General Discussion..... | 26 |
| 6. Conclusions..... | 29 |
| References..... | 30 |
| Figure Sources..... | 31 |
| Appendix A: Grid Patterns for the Theoretical Mesh Models..... | 32 |
| Appendix B: Theoretical Experiment Results..... | 34 |
| Appendix C: Practical Experiment Raw Testing Data..... | 42 |

List of Figure

| | |
|--|----|
| Figure 1: The 1988 America's Cup Match, NZ (far) vs USA (near) ^A | 2 |
| Figure 2: (Clockwise from top left): USA 17 with its traditional soft sail ^B , USA 17 with the wing mast and sail ^C , USA 17 and Alinghi 5 racing in the 2010 America's Cup ^D | 3 |
| Figure 3: Vestas Sail Rocket on its record run ^E | 4 |
| Figure 4: Principle forces on a sailboat..... | 6 |
| Figure 5: Flow over an air foil ^F | 8 |
| Figure 6: Apparent wind and true wind geometry..... | 9 |
| Figure 7: Pressure distribution at 14° angle of attack and 10 m/s for a wing (left) and a traditional sail (right)..... | 15 |
| Figure 8: Flow Velocity at 14° angle of attack and 10 m/s for a wing (left) and a traditional sail (right)..... | 15 |
| Figure 9: Pressure distribution at 0° angle of attack and 10 m/s for a wing (left) and a traditional sail (right)..... | 16 |
| Figure 10: Flow Velocity at 0° angle of attack and 10 m/s for a wing (left) and a traditional sail (right)..... | 16 |
| Figure 11: RC radio and RC Laser (not to scale)..... | 19 |
| Figure 12: Servos and battery pack for the RC Laser..... | 20 |
| Figure 13: Wing sail (left) and traditional sail (right) used for the testing..... | 21 |
| Figure 14: Testing on Spreckles Lake, traditional sail (left) and wing sail (right)..... | 22 |
| Figure 15: Compass rose of sailing relative to the wind ^G | 23 |
| Figure 16: Testing data from experimental tests..... | 24 |
| Figure 17: Testing data from experimental tests with normalization of the wing sail data on starboard..... | 25 |
| Figure 18: Two section camber wing cross-section..... | 27 |
| Figure 19: Oracle Team USA, winner of the 34th America's Cup with their cambered wing main sail ^H | 28 |
| Figure 20: Grid mesh for wing sail section with 14 degrees angle of attack..... | 32 |
| Figure 21: Grid mesh for traditional sail section with 14 degrees angle of attack..... | 32 |
| Figure 22: Grid mesh for wing sail section with 0 degrees angle of attack..... | 33 |
| Figure 23: Grid mesh for traditional sail section with 0 degrees angle of attack..... | 33 |
| Figure 24: Pressure distribution at 14° angle of attack and 100 m/s for a wing (left) and a traditional sail (right)..... | 34 |
| Figure 25: Flow Velocity at 14° angle of attack and 100 m/s for a wing (left) and a traditional sail (right)..... | 34 |
| Figure 26: Pressure distribution at 14° angle of attack and 50 m/s for a wing (left) and a traditional sail (right)..... | 35 |
| Figure 27: Flow Velocity at 14° angle of attack and 50 m/s for a wing (left) and a traditional sail (right)..... | 35 |
| Figure 28: Pressure distribution at 14° angle of attack and 20 m/s for a wing (left) and a traditional sail (right)..... | 36 |
| Figure 29: Flow Velocity at 14° angle of attack and 20 m/s for a wing (left) and a traditional sail (right)..... | 36 |
| Figure 30: Pressure distribution at 14° angle of attack and 10 m/s for a wing (left) and a traditional sail (right)..... | 37 |
| Figure 31: Flow Velocity at 14° angle of attack and 10 m/s for a wing (left) and a traditional sail (right)..... | 37 |
| Figure 32: Pressure distribution at 0° angle of attack and 100 m/s for a wing (left) and a traditional sail (right)..... | 38 |
| Figure 33: Flow Velocity at 0° angle of attack and 100 m/s for a wing (left) and a traditional sail (right)..... | 38 |
| Figure 34: Pressure distribution at 0° angle of attack and 50 m/s for a wing (left) and a traditional sail (right)..... | 39 |
| Figure 35: Flow Velocity at 0° angle of attack and 50 m/s for a wing (left) and a traditional sail (right)..... | 39 |
| Figure 36: Pressure distribution at 0° angle of attack and 20 m/s for a wing (left) and a traditional sail (right)..... | 40 |
| Figure 37: Flow Velocity at 0° angle of attack and 20 m/s for a wing (left) and a traditional sail (right)..... | 40 |
| Figure 38: Pressure distribution at 0° angle of attack and 10 m/s for a wing (left) and a traditional sail (right)..... | 41 |
| Figure 39: Flow Velocity at 0° angle of attack and 10 m/s for a wing (left) and a traditional sail (right)..... | 41 |

List of Tables

| | |
|---|----|
| Table 1: Summary of force outputs on selected theoretical models..... | 14 |
| Table 2: Practical experiment testing data..... | 42 |

List of Nomenclature

| | |
|----------------|--|
| a | = Speed of sound |
| C | = Constant |
| C_D | = Coefficient of drag |
| C_L | = Coefficient of lift |
| CL | = Centerline of the boat |
| E | = Energy |
| e | = Total energy |
| $F_{C/K}$ | = Centerboard/Keel force on the sailboat |
| $F_{D/K}$ | = Drag force on the keel/centerboard foil |
| $F_{D,S}$ | = Force of drag on the sail |
| F_{Drive} | = Drive force on the sailboat |
| $F_{L/K}$ | = Lift force on the keel/centerboard foil |
| $F_{L,S}$ | = Force of lift on the sail |
| F_R | = Resistance force on the sailboat |
| $F_{Righting}$ | = Righting force on the keel/centerboard foil (counter to the sail) |
| F_{Sail} | = Force of the sail on the sailboat |
| L/D | = Lift to drag ratio |
| Pr | = Prandtl number |
| q_{max} | = Maximum energy flux |
| \Re | = Reynolds number |
| S | = Cross sectional area of the foil |
| u, v | = Flow velocity vector field (Cartesian velocities) |
| V | = Velocity of the air around the foil |
| V_B | = Velocity of the boat |
| V_R | = Velocity of the true wind |
| V_T | = Velocity of the apparent wind |
| γ | = Ratio of specific heats (typically 1.4) |
| γ_R | = Relative wind direction |
| γ_T | = True wind direction |
| λ | = Leeway angle (angle the boat is moving through the water relative to centerline) |
| μ | = Dynamic viscosity |

ρ = Density

∇ = Nabla operator

1. Introduction

1 History of the America's Cup and Wing Sails

The America's Cup is the most prestigious trophy in all of the sport of sailing. It has been contested 34 times with the first competition taking place in 1851. This also makes the America's Cup the oldest trophy in international sport. The America's Cup regattas have for the most part been a series of one-on-one match races between two competing sailboats, the defender and the challenger. Each competing syndicate is responsible for the design and construction of their individual yacht. While the yachts are not identical, they are all bound by a set of pre-determined design rules for each individual match to help ensure that the racing would be relatively even. Because of this, the design of the boats has always been just as important, if not more important than the people sailing the boats.

In the very first match, in 1851, the Royal Yacht Squadron in Cowes, England invited yachts to compete in a race around the Isle of Wight for the "R.Y.S. £100 Cup". John Stevens and a small group of other Americans decided to build a boat that would race in this event. They built the schooner, *America*, which won the race. Thereafter the trophy was renamed as the America's Cup after the yacht which first won the trophy. Between 1851 and 1983, the New York Yacht Club enjoyed the longest winning streak in sports history, successfully defending the cup 23 times. In 1983, under a shroud of secrecy on the design of the boat, *Australia II*, Alan Bond and his syndicate from Australia defeated the New York Yacht Club for the America's Cup. The yacht that the Australians used had a design feature that had never been seen before, a winged keel (a keel is an underwater appendage used to provide righting moment for sailboats to counter the force of the wind on the sails). This winged keel allowed *Australia II* to sail much faster than the American yacht *Liberty* on certain points of sail. After helping the Australians win the cup, the design innovation led to winged keels becoming commonplace for yacht designs of all sizes today.



Figure 1: The 1988 America's Cup Match, NZ (far) vs USA (near) ^A

Another large leap in sailing technology took place only 5 years later. First, in 1987, a team from San Diego Yacht Club skippered by Dennis Connor (the same skipper who lost the cup in 1983) went down to Fremantle, Australia and won the cup back for the United States. Then in 1988, a team from New Zealand challenged for the America's Cup seemingly out of nowhere in what is called a "Deed of Gift" match. A Deed of Gift match is essentially one club challenging another without a challenger selection series. The New Zealanders had built a 90 foot mono-hull boat (as the deed of gift for the trophy stated) and were ready to take on the American team from San Diego Yacht Club. Dennis Connor decided that he did not

have enough time to build a competitive big boat so it was decided to build a multi-hull catamaran for the racing. Dennis and his syndicate had one more trick up his sleeve. They hired some of the greatest airplane designers around (names such as Burt Rutan) to design a hard wing to be used as a sail in place of the traditional soft sails made mostly out of Kevlar and Dacron. They tested between the soft traditional sail and the wing sail and found that the wing sail was far superior to the soft sail on all points of sail. The match was not even close; with the wing sail catamaran beating the large mono-hull boat with a soft sail by about 20 minutes each race. The fact that the races were so one sided led the New Zealanders to take the matter to court, with the courts ultimately deciding that because the Deed of Gift for the America's Cup had no specifications about the boat other than it is to be contested in boats 90 feet or less with one mast, the catamaran with the wing mast was legal.

Due to the long court battles over the validity of the boats, the next 5 America's Cups (1992-2007) were contested in very similar mono-hull boats that all conformed to a design rule. After the 2007 America's Cup, there was another legal battle brewing over the rules for the next America's Cup match. In the end, another Deed of Gift match was set for 2010 between the challenger, BMW Oracle from the Golden Gate Yacht Club in the United States and the Defender Alinghi from Société Nautique de Genève in

Switzerland. Because of the last America's Cup Deed of Gift match in 1988 being so one sided in favor of the multi-hull boats, both teams set off to build multi-hull boats for the match.

For the 2010 America's Cup, the defender Alinghi built a 110 foot long two hulled catamaran, *Alinghi 5*, with a traditional soft sail plan (approximately 21,800 square feet of sail area). With so much sail area (power) and so little amount of boat in the water (drag), *Alinghi 5* was able to sail at twice the speed of the wind going upwind and 2.5 times the speed of the wind downwind. The challenger, BMW Oracle Racing built a 113 foot three hulled tri-maran, *USA 17*, also with a traditional soft sail plan when it was first launched. There were rumors circling before the event that BMW Oracle Racing had something up their sleeve and in 2009 a year before the match, they announced that they had developed a rigid wing sail to replace the traditional soft main sail that was currently on the boat. The wing that was unveiled for the boat was originally a 190 foot tall wing which then grew after modifications to a 223 foot wing (longer than the entire wingspan of a Boeing 747). With the wing sail, *USA 17* could sail over 3 times the speed of the wind on all points of sail.



Figure 2: (Clockwise from top left): USA 17 with its traditional soft sail ^B, USA 17 with the wing mast and sail ^C, USA 17 and Alinghi 5 racing in the 2010 America's Cup ^D

On February 10, 2010, the first race of the 33rd America's Cup took place in Valencia, Spain. It was clear from the start of the race that BMW Oracle Racing and *USA 17* had a clear speed advantage on all points of sail. They ended up beating *Alinghi 5* by over 8 minutes in the first race of a best of 3 match. The second race was more of the same with *USA 17* actually trailing for a bit due to a bad start but just flying past *Alinghi 5* on the first leg of the race and going on to a win of over 5 minutes. The America's Cup was heading back to America for the first time since 1995 and it was mostly due to the design innovation of the wing sail.

The speeds exhibited by *USA 17* in the 33rd America's Cup have had a lasting impression on how the boats of the future should be designed. For the 34th America's Cup in 2013 as well as the 35th Cup coming in 2017, the design rule for the competing boats incorporated a wing sail similar to the one used by *USA 17* but on a much smaller scale. The boats were reaching top speeds of over 45 miles per hour in only 20 miles per hour of wind. Just as the winged keel became a standard for high performance boats after the 1983 America's Cup, the wing sail is now becoming the standard for many different types of high performance boats.

2 Other Uses of Wing Sails in Sailing Endeavors



Figure 3: *Vestas Sail Rocket* on its record run^E

Another usage of a wing sail to achieve higher performance than a traditional soft sail was on a boat called *Vestas Sail Rocket*. It was created for the purpose of breaking the world speed record for a wind powered craft on the water. Prior to the construction of the boat, the record was held by a kite board at just over 50 knots (57 mph). The *Vestas Sail*

Rocket, with its wing sail and low profile smashed the record as it ran the 500m course at 65.45 knots (75.32 mph) with a 68.01 knots (78.26 mph) peak in only 30 mph of wind. This record would not have been possible without the wing sail on the boat.

Sails have also become a topic of discussion on how to reduce carbon emissions by ocean going freighters around the world. Almost all commodities that are moved between countries are moved on container ships. Currently, there are over 10,000 ships worldwide that are moving goods via cargo containers and almost 5000 tanker ships (such as oil tankers) in operation. Most of those vessels are burning fossil fuels such as petrol and oil to operate and their exhaust is polluting the Earth. There is current research out there that would help reduce the dependency on fossil fuels by placing sails on these large vessels and letting the wind help propel them around the world. The research is centering around optimizing wing sail design for large ships in differing sail patterns (amount of sails on the ship). If this research can help stem the use of fossil fuels, then it is very worthwhile.

Sailing and sail technology also has applications in the Aerospace Engineering field in the form of Atmospheric Satellites. The concept uses two aircraft tethered together where they use each other for both propulsion and stability, similar to how a boat uses a sail to maneuver through the water. The satellite body acts as the sail in this application. This theory uses modern sailing principles to help solve the problem of how to stabilize and propel the atmospheric bodies as a system.

Using a solar sail as a means of spacecraft propulsion is another area that uses modern sailing principles for propulsion. The basic theory is that the sun radiates photons in what is called a solar wind. Sails that are deployed on spacecraft use this solar wind just as a sailboat would use the wind on earth to propel the sail. Most of the development and testing of solar sails has been with traditional films deployed on rigid members similar to how sails are deployed on sailboat masts on Earth but with the increasing knowledge about wing sails, more rigid solar sails are being looked at as possible alternatives.

3 Motivation for Project

Prestigious regattas such as the America's Cup and the World Sailing Speed Record have throughout their history pushed the creative minds of designers. Many of the design innovations such as the development of wing sails created in the quest for victory have become commonplace in not only the

sailing industry, but other industries as well. With modern sailing principles becoming helpful in solving modern engineering problems, it is worth investigating if the gains of using a wing sail versus a traditional soft sail can be seen on smaller sized boats than those of the America's Cup at lower wind speeds.

2. Forces Acting on a Sailboat and its Sail

When most people envision a sailboat sailing through the water, they picture the sail catching the wind and pushing the boat forward. If this were true, then how would a sailboat be able to sail into the wind or even with the wind at its side? The solution is in the forces and the force balance acting on the sailboat and the sails. The principle forces acting on a sailboat are the centerboard/keel force, the sail force and the resistance force. Other forces acting on a sailboat that are not shown (they are small and considered negligible) include the weight of the crew in the boat which is counter balanced by the hull force floating in the water (or displacement). All of these force vectors are added up to create the drive force or direction of motion. When the boat is moving at a constant velocity, the drive force is equal to zero (no acceleration) and the sum of all of the forces on the boat also equals zero.

$$F_{Drive} = F_{C/K} + F_{Sail} + F_R$$

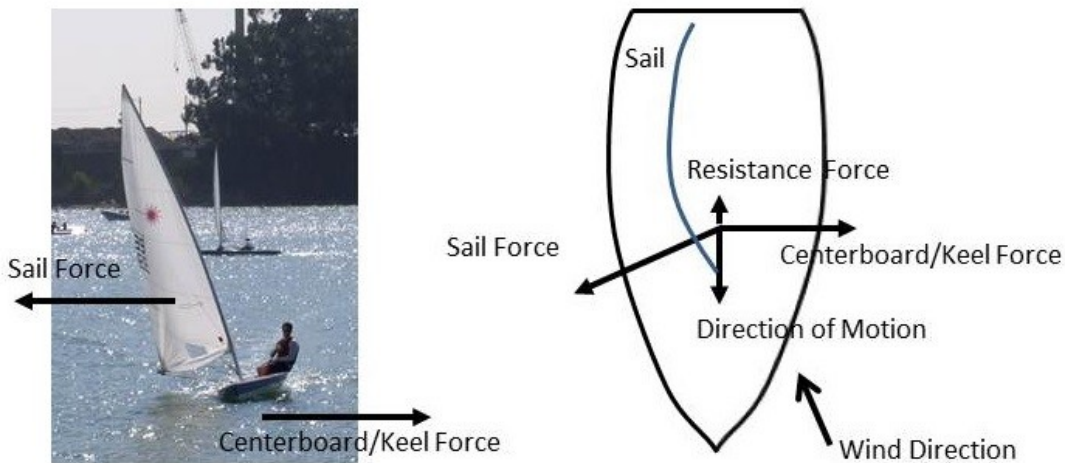


Figure 4: Principle forces on a sailboat

The centerboard/keel force, $F_{C/K}$ is a force that is provided by the appendage on the boat that is below the hull of the boat. If there was no centerboard/keel on the boat, that boat would just slip sideways through the water and would not go forwards. This is due to two factors. As the sail force pushes the boat over with a moment about the center of gravity of the boat, the centerboard/keel provides a counter force opposite of the sail. The second factor is that the centerboard/keel also acts similar to an airfoil, specifically similar to a glider because of the low angle of attack in relation to the flow of the substance and also the size of the foil compared to the density of the fluid it is moving through. The density of the water is much higher than that of air so the centerboard/keel can be relatively small yet provide the necessary force to balance the sail force. Centerboard/keels are typically symmetrical about the chord length in order to be useful in multiple directions. The force acting on the centerboard/keel, $F_{C/K}$ can be broken down into the three components: $F_{L,K}$, the force of lift on the foil, $F_{D,K}$, the drag force of the foil moving through the water and $F_{Righting}$, the righting force that counters the force of the sail.

$$F_{C/K} = F_{L,K} + F_{D,K} + F_{Righting}$$

The resistance force, F_R is the amount of drag caused by the boat moving through the water. This force consists of many different components including the skin friction of the boat moving through the water, the form drag or drag due to the shape of the boat, and the wave making drag force. There are other forces that act on a boat but these are negligible if a boat moves in a straight line along its longest dimension. The largest component of the resistance force is the wave making drag force. At lower speeds, boats displace the water they sail through as they move the water molecules around them. This creates a drag on the boat that is proportional to the speed of the boat. Once a boat reaches its hydrodynamic hull speed, it enters a forced mode where the drag on the boat is increasing exponentially as the speed only slightly increases. At higher speeds, certain hull shapes actually allow a boat to enter a turbulent and laminar flow called planing which allows the resistance force to increase at a slower rate than if the boat was just displacing water.

Opposite of the resistance force is the drive force, F_{Drive} or direction of motion. This is the sum of all of the other forces and makes the boat accelerate in a given direction. If a boat is moving at a constant velocity and there is no acceleration, then the drive force is zero and the rest of the forces added together equal zero.

$$F_{Drive} = F_{C/K} + F_{Sail} + F_R = 0 \quad (\text{constant boat velocity})$$

The sail force, F_{Sail} is the force applied by the wind moving over the sails. The sail force acting on a sailboat is created by air movement near and relative to the sails causing air pressure differences and air viscosity acting near the sail.

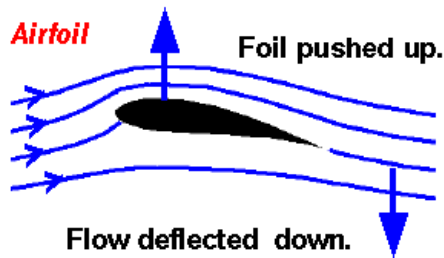


Figure 5: Flow over an air foil ^F

At most points of sail, the sail acts as an airfoil with pressure differences on the top and bottom of the sail. The forces can be summed up into a simple formula for the entire surface.

$$F = CE$$

Using the Bernoulli equation for kinetic energy, the maximum force over the entire sail can be shown.

$$E = q_{max} S = \frac{1}{2} \rho S V^2$$

Where the full expression for the sail force can be described as.

$$F_{Sail} = \frac{1}{2} \rho S C V^2$$

The velocity component V for the sail force equation above is represented by the flow of wind over the sail. Since sails (wing or traditional) are also moving forward due to being attached to the boat, the true wind velocity vector, V_T , seen if standing on shore is not the one that that boat sees. The boat

instead sees a relative wind velocity vector of, V_R . The relationship between true wind velocity and relative wind velocity can be shown in figure 6 below. Note that as the speed of the boat increases, the angle of the apparent wind gets smaller and the length of the V_R vector gets larger.

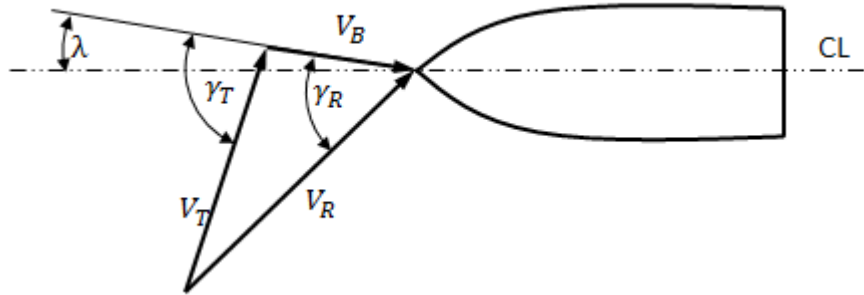


Figure 6: Apparent wind and true wind geometry

For each sail force F_{Sail} , there is a component of the force in each of the three principle directions. The x component of the force is the axis that is parallel to the direction of the particle's movement. This component is also known as the drag ($F_{D,S}$) and the C for the equation can be known as C_D .

$$F_{D,S} = \frac{1}{2} \rho S C_D V^2$$

The z component of the force is the axis perpendicular to the direction of movement of the particles along the sail and also perpendicular to the wing span of the sail. This component is also known as lift ($F_{L,S}$) and the C for the equation can be known as C_L .

$$F_{L,S} = \frac{1}{2} \rho S C_L V^2$$

The last component is the y axis along the span of the wing and for a sail/wing profile of infinite length (where the 2D representation of the foil holds true), it is zero. In our case, we are theoretically comparing infinite wingspan shapes.

Using the Bernoulli equation, we discover that changing the coefficients of lift and drag can have a big effect on the sail force acting on a sailboat. Increasing the lift on the boat would provide more force for the

boat to move forward. Also, decreasing the drag on a sailboat would also provide more force for the boat to move forward. Because of this relationship, a common variable used in sail making (and also air foil design) is the lift to drag ratio (L/D).

$$L/D = C_L / C_D$$

The lift to drag ratio for most air foils is known for certain angles of attack and is typically plotted on a polar curve. For the purposes of this analysis, the drag will remain relatively constant and variations in lift will be investigated.

When investigating wing sails and traditional sails, we are going to be looking to increase the lift generated on the sail/wing which then in turn would increase the overall sail force and allow the boat to move through the water faster. There are three ways to increase the lift on the craft from the Bernoulli equation derived above. We can change the density of the fluid that the air foil moves through, we can also increase the velocity that the air foil is moving in and lastly we could alter the surface area of the foil to increase the lift. Changing the shape of the sail from the traditional soft sail to the wing sail could provide more lift and therefore more speed for the boat.

3. Theoretical Analysis of Traditional Sails and Wing Sails

4 Computational Fluid Dynamics Theory

In order to theoretically examine the differences between a traditional sail and a wing sail, a Computational Fluid Dynamics (CFD) solver must be used. Computational Fluid Dynamics uses numerical methods to solve problems that involve fluid flow. CFD solving programs utilize different methods in order to solve Navier-Stokes equations or Euler equations. These use conservation laws (mass, momentum, and energy).

The conservation of mass states that over a given system, the amount of mass in the system remains unchanged. The law implies that mass in the system can neither be created nor destroyed. Specific to

fluid dynamics, the conservation of mass in a system means that the amount of fluid going into the system has to be equal to the amount of fluid going out of the system. It can be written in differential form as the following equation.

$$\frac{\partial \rho}{\partial t} + \nabla \cdot (\rho \mathbf{u}) = 0$$

The conservation of momentum takes into account Newton's second law of motion and states the amount of momentum in a given system must remain unchanged. For fluid dynamics it means that any change in momentum in the system be due to the fluid flow into the system and the net forces that are acting within that system. The equation for fluid dynamics takes the following form.

$$\frac{d\mathbf{u}}{dt} = \vec{F} - \frac{\nabla p}{\rho}$$

The conservation of energy states that over a given system, the total amount of energy in the system is constant and does not change. Energy may take different forms but the total amount of energy is unchanged for the system. For fluid dynamics, the second law of thermodynamics requires that the dissipation of the system is always positive or energy cannot be created through viscosity. The equation can be expressed as below.

$$\rho \frac{dh}{dt} = \frac{dp}{dt} + \nabla \cdot (k \nabla T) + \Phi$$

These equations in non-dimensional form are:

$$\partial_t Q + \partial_x E + \partial_y F = \Re^{-1} (\partial_x E_v + \partial_y F_v)$$

where

$$Q = \begin{bmatrix} \rho \\ \rho u \\ \rho v \\ e \end{bmatrix}, \quad E = \begin{bmatrix} \rho u \\ \rho u^2 + p \\ \rho uv \\ u(e + p) \end{bmatrix}, \quad F = \begin{bmatrix} \rho v \\ \rho uv \\ \rho v^2 + p \\ v(e + p) \end{bmatrix}, \quad E_v = \begin{bmatrix} 0 \\ \tau_{xx} \\ \tau_{xy} \\ f_4 \end{bmatrix}, \quad F_v = \begin{bmatrix} 0 \\ \tau_{xy} \\ \tau_{yy} \\ g_4 \end{bmatrix}$$

with

$$\tau_{xx} = \frac{\mu(4u_x - 2v_y)}{3}$$

$$\tau_{xy} = \mu (u_y + v_x)$$

$$\tau_{yy} = \frac{\mu (-2u_x + 4v_y)}{3}$$

$$f_4 = u \tau_{xx} + v \tau_{xy} + \mu Pr^{-1} (\gamma - 1)^{-1} \partial_x a^2$$

$$g_4 = u \tau_{xy} + v \tau_{yy} + \mu Pr^{-1} (\gamma - 1)^{-1} \partial_y a^2$$

Pressure in the system is related to the conservative flow variables by the equation of state as shown below

$$p = (\gamma - 1) \left(e - \frac{1}{2} \rho (u^2 + v^2) \right)$$

Typically, the ratio of specific heats γ is 1.4 and the speed of sound, a , and the dynamic viscosity μ are constants derived for the system. For Euler equations, there are no viscous influences and therefore the right side of the first equation ($\Re^{-1} (\partial_x E_v + \partial_y F_v)$) can be set to zero to form the equations.

5 Theoretical Experiment Setup

The ESI Group makes a suite of CFD software designed to analyze geometric shapes called the ACE+ Suite. The ACE+ software suite includes a geometry modeler, a CFD solver and also a CFD model viewer which allow the user to properly simulate complex aerospace problems that might arise. The software is capable of demonstrating CFD solutions by using a density based compressible Euler and Navier-Stokes flow solver with moving multi-body dynamics, generalized finite rate chemistry and thermal non-equilibrium modules.

For this application, a simple sail geometry was made showing a similar curvature on both sides of the sail. The shape of the sail is non-linear and has a very thin rectangular leading and trailing edge (for simplicity). A similar shape was created for the wing sail with the only difference being that the lower edge of the wing was linear in shape. This allows the comparison of similar chord lengths and geometric shapes with the only difference being the lower edge as a sail or a wing. Two different angles of attack

were used for the testing, one at 14 degrees (typical for a boat on a reaching course) and 0 degrees (for reference).

To accurately display the velocity and pressure profiles, a grid mesh was used on the models created in ESI. The mesh gets more detailed (less area per cell) as you get closer to the wing or sail shape in order to more precisely portray what is going on around the shape. A meshing pattern with the power of 2 was used close to the shape for this experiment. The meshing patterns for both the traditional and wing sail at both 14 and 0 degrees angle of attack are shown in Appendix A.

For the testing setup, an inlet was placed on the left side of the sail/wing and an extrapolated outlet was placed on the right side. The inlet and the initial conditions for this test were at the flow velocity noted, 1 atm and 300K. A Navier-Stokes set of equations was used in the theoretical simulations shown on 1000 cycles with all other values set to default (per the program) unless otherwise noted.

For the testing four different flow velocities were used for each angle of attack to demonstrate the flow profiles at different Reynold's Numbers. The four flow velocities chosen were 100, 50, 20 and 10 m/s. The 100 and 50 m/s flow velocities are well out of the scope of the principle being tested in this paper but were used more to calibrate the results and ensure that the data output was correct. The 10 m/s flow velocity is a very realistic example of the velocity a small sailboat can see while out sailing and is a good representation.

6 Results of Theoretical Experiment

Running the FASTRAN solver from ESI for each simulation gives us two outputs of note, a visualization where the user can show the pressure and flow profiles of each simulation and also a force file which outputs the forces acting on the set boundaries for each section within the simulation. Table 1 shows a summary of the outputs of the force file for this simulation. The angle of attack, cross section and flow velocity are given from the inputs into the system. The vertical and horizontal forces are outputs of the force file. The lift force, drag force and lift to drag ratio (L/D) are calculated from the vertical and horizontal

forces on the system. The negative signs in the data on Table 1 reflect the direction of the vectors and do not mean that the section is producing a negative amount of force because that is not possible.

Table 1: Summary of force outputs on selected theoretical models

| Angle of Attack (degrees) | Cross Section | Flow Velocity (m/s) | Vertical Force Under (N) | Vertical Force Over (N) | Lift Force (N) | Horizontal Force Before (N) | Horizontal Force After (N) | Drag Force (N) | L/D Ratio |
|----------------------------------|----------------------|----------------------------|---------------------------------|--------------------------------|-----------------------|------------------------------------|-----------------------------------|-----------------------|------------------|
| 0 | Sail | 10 | 494290 | -494310 | 20 | 3106.3 | -3078.5 | 27.8 | 0.72 |
| 0 | Wing | 10 | 494330 | -494300 | 30 | 3105.1 | -3080.1 | 25 | 1.20 |
| 14 | Sail | 10 | 494150 | -494990 | 840 | 3079.2 | -3111.1 | 31.9 | 26.33 |
| 14 | Wing | 10 | 494170 | -494940 | 770 | 3082 | -3106.9 | 24.9 | 30.92 |

The visualization output from the ESI software allows the user to pictorially demonstrate the results of the simulation that was run. The software allows the user to show pressure distributions, flow profiles and other useful factors. For each angle of attack (0 and 14 degrees) and flow velocity (100, 50, 20 and 10 m/s), both a traditional sail profile and a wing sail profile were run and placed side by side in the visualization software for easy comparison. For each of the simulations, both a pressure distribution and a flow velocity figure were created. The pressure distribution shows how the flow creates variable pressure around the given geometry. The flow velocity shows how the flow interacts with the geometry given in the simulation. The visualization software also has adjustable scales which were shown on the figures to give a quantity to the colors in the output. The scales were normalized from the default settings in order to quickly and accurately compare the data. Every simulation output created with the visualization software is available for viewing in Appendix B at the end of this paper.

Figures 7 and 8 show the pressure distribution and flow velocity profile respectively for a 10 m/s flow velocity and a 14 degree angle of attack. The wing sail is on the left of each figure and the traditional sail is on the right. The pressure and velocities have been set equal for both sides of each figure to accurately compare the data for each sail.

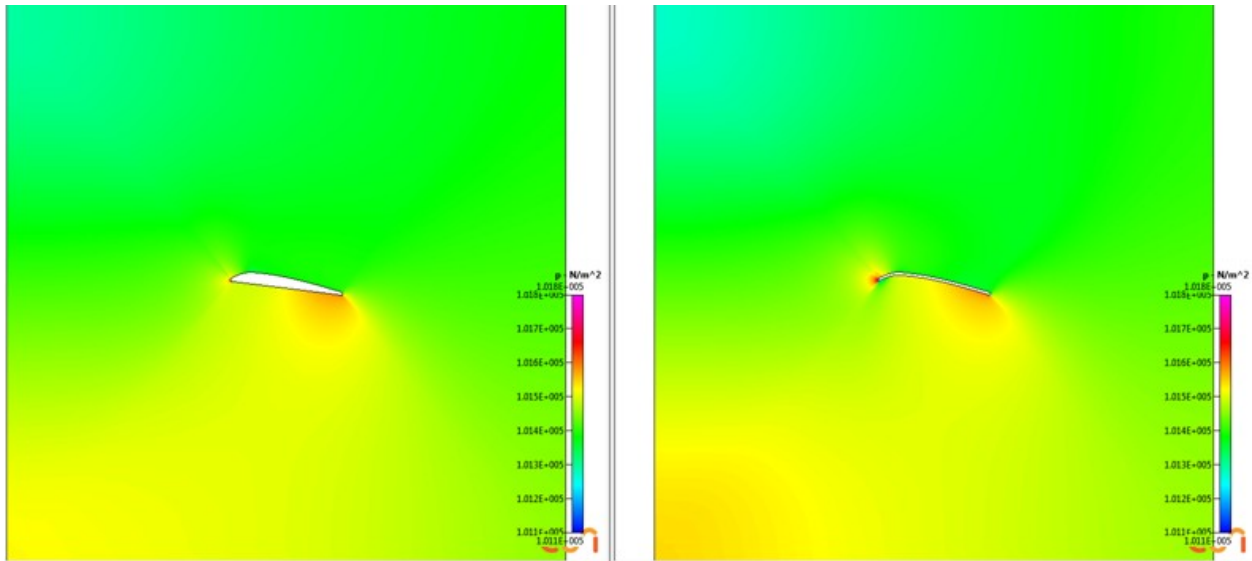


Figure 7: Pressure distribution at 14° angle of attack and 10 m/s for a wing (left) and a traditional sail (right)

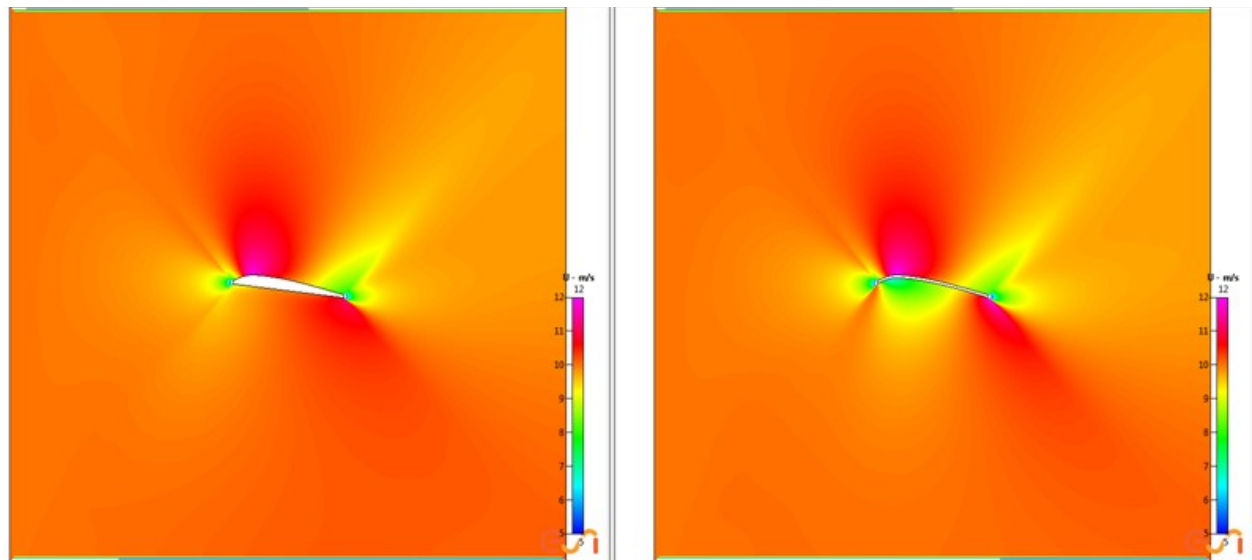


Figure 8: Flow Velocity at 14° angle of attack and 10 m/s for a wing (left) and a traditional sail (right)

Figures 9 and 10 show the pressure distribution and flow velocity profile respectively for a 10 m/s flow velocity and a 0 degree angle of attack. All figures have the wing sail on the left and the traditional sail on the right. The pressure and velocities have been set equal for both sides of each figure to accurately compare the data for each sail.

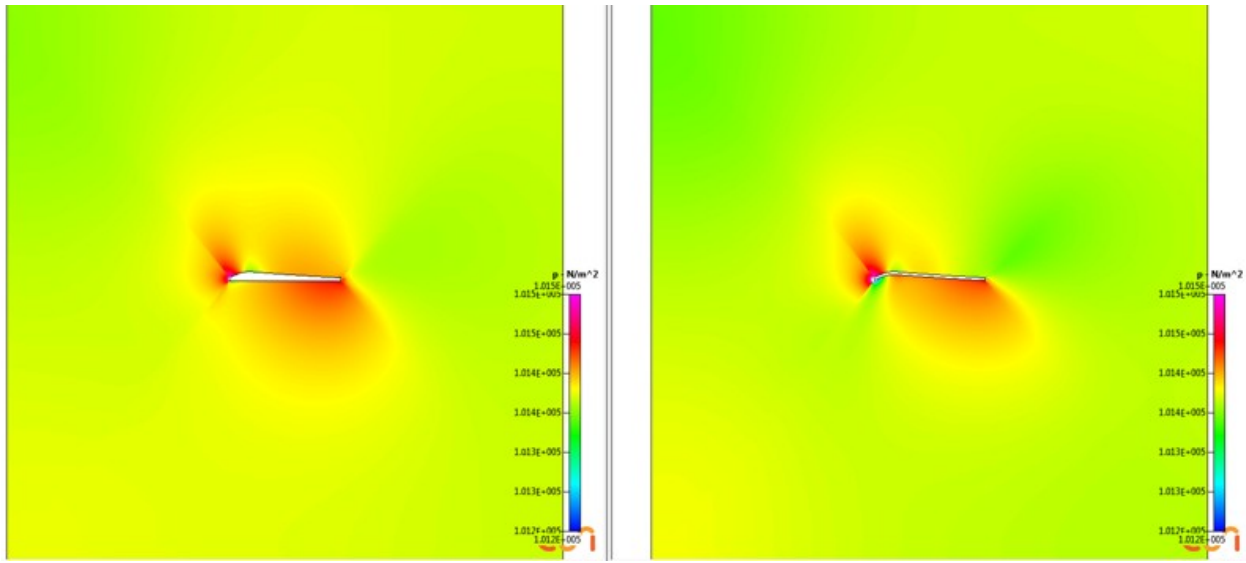


Figure 9: Pressure distribution at 0° angle of attack and 10 m/s for a wing (left) and a traditional sail (right)

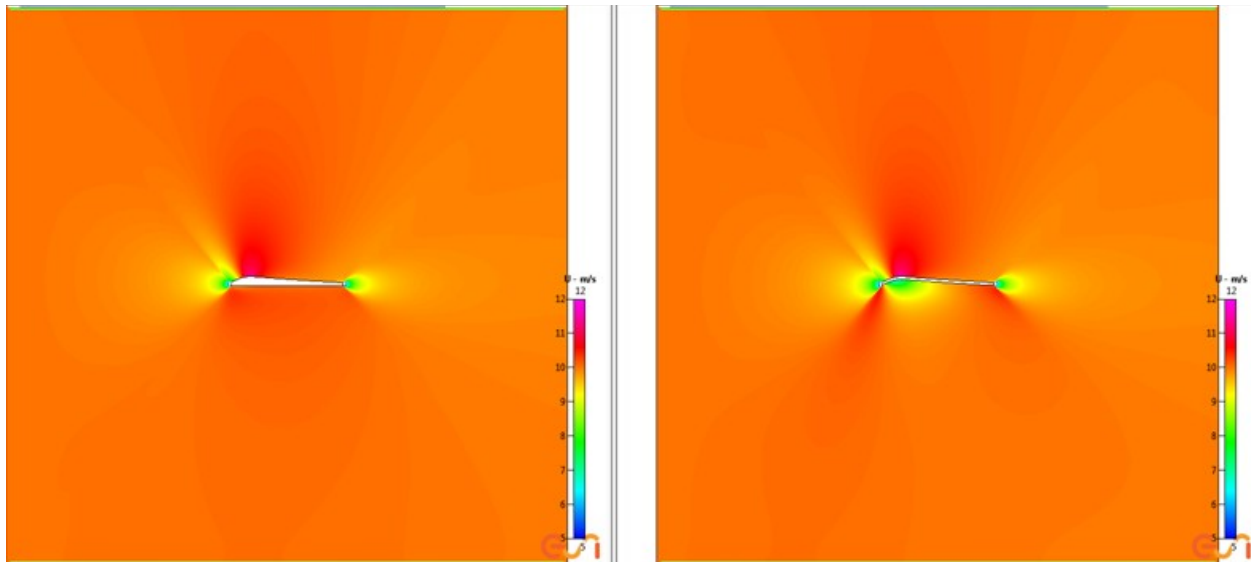


Figure 10: Flow Velocity at 0° angle of attack and 10 m/s for a wing (left) and a traditional sail (right)

7 Discussion of Theoretical Experimental Analysis

For the 14 degrees angle of attack, the wing and the traditional sail have a very similar pressure distribution as seen in Figure 7. Both shapes have higher pressure on the underside of the shape as expected to produce lift on the body. Both shapes also have a higher pressure at the tail end of the body. The traditional sail has a slightly higher pressure on the very front edge than the wing and also a small area of lower pressure on the front part of the lower side of the sail. This is most likely due to the fact that the angle of attack is not steep enough for the flow of particles to maneuver around the front edge of the sail cleanly. This is shown well in Figure 8 as the sail has a large area of lower flow around the front edge of the sail on the lower side. The flow velocity for both the wing and the traditional sail in Figure 8 is mostly the same (except for the previously mentioned flow matter) with a higher velocity on the upper side as expected showing the lift on the body. It is worth noting that while both seem to be generating lift; the wing seems to have a more even distribution of flow velocity and pressure distribution than the traditional sail.

In Table 1, we see that for the 14 degree angle of attack force output files, the traditional sail actually produces slightly more lift than the wing sail. This is offset, however, by the fact that the traditional sail produces more drag than the wing section and therefore has a lower lift to drag ratio (L/D ratio). The wing section, with its lower drag than the sail section has a higher lift to drag ratio and therefore is the more efficient sail to use in the conditions provided for this part of the experiment.

For the 0 degrees angle of attack, the wing and traditional sail once again have very similar pressure distribution profiles (Figure 9). Both shapes have higher pressure on the underside of the shape to produce the expected lift on the sail. The traditional sail has a slightly greater pressure difference between the top and bottom sides near the trailing edge of the sail but this is most likely offset by the appearance once again of an area of very low pressure at the very front edge of the shape. The wing section has a much smoother pressure distribution than the traditional sail and similarly has a smoother flow distribution

as seen in Figure 10. For the traditional sail, the flow is once again interrupted by the front edge of the shape and causes a very low flow situation. Both the wing and traditional sail have low flow around the very front edge and trailing edge of the shapes and this is expected because the flow is perpendicular to the section and has a hard time moving around the shape efficiently. The flow around the top of both the wing and traditional sail are close to being the same so the difference in lift and drag developed by the sections comes down to the bottom side and how the air moves around it.

As you can see in Table 1, the amount of lift produced by both the wing and the traditional sail is much lower than at 14 degrees angle of attack. This is expected as any angle of attack would provide more lift as the air flows around the surface. The wing has a slightly higher amount of lift developed than the traditional sail and once again has a lower drag force than the sail section. This is most likely due to the front edge of the traditional sail and the lack of pressure and flow around it. The wing section, just as in the 14 degree angle of attack has a higher lift to drag ratio than the traditional sail and is the more efficient section for this experiment.

4. Practical Experimental Analysis of Traditional Sails and Wing Sails

8 Practical Experimental Setup

To experimentally test the performance of traditional sails and wing sails, we must find a testing platform that allows for all performance factors besides the sail and wing itself to be controlled. To do this, a radio controlled sailboat called an RC Laser was chosen to be the testing boat. The RC Laser is a 1/4 scale radio controlled model of the Laser sailboat that is one of the boats contested in the Olympic Games since 1996. The RC Laser is a simple hull design with a single sail mounted on a mast with a very minimal amount of control lines for the sail (to adjust the shape of the sail). The simplicity of the RC Laser allows a wing sail to be fitted to the hull without changing a lot of factors on the boat and its performance.



Figure 11: RC radio and RC Laser (not to scale)

The RC Laser hull is made out of a plastic composite material and is formed in a mold to keep the boats similar coming out of the factory. On board the boat is a battery pack which powers the radio remote. The radio remote has two channels that control the two servos on the boat. One servo controls the rudder at the back of the boat for steering and the other servo controls how far the sail goes in and out (otherwise known as the mainsheet). The boat also has a fiberglass keel with a lead bulb to provide both the keel force and also to provide righting moment to the boat. The mast for the sail is made out of two pieces of composite fitted together that slides into a hole on the hull of the boat which allows it to rotate around. On the mast is the connection for the boom, otherwise known as the gooseneck. The boom is an aluminum tube which runs along the bottom of the sail and has sliders on it. The sliders connect to the clew or aft bottom section of the sail to the boom and also connect the boom to the mainsheet which allows for control of the sail. The traditional sail for the boat has a sleeve on it where the mast slides in and also a grommet at the clew for the slider connection. The traditional sail has a sail area of approximately 710 in². The controller for the RC Laser is a four channel controller (two channels unused) that has both fine tune and coarse tune adjustments for both servos.



Figure 12: Servos and battery pack for the RC Laser

For the wing sail, a lightweight yet strong material needed to be used that could also be relatively the same size as the traditional sail on the RC Laser. A standard balsa wood glider kit was procured for the construction of the wing sail. The glider wingspan was slightly longer than the length of the mast of the RC Laser so the wing was sized to fit the mast instead of the nominal wingspan that the kit calls for. The standard glider kit also calls for the wing to be swept up at the wingtips but this was not done for the wing sail as it would not be similar to the straight mast of the traditional sail. The wing structure was constructed using the kit directions (other than the modifications mentioned) and the mast for the RC Laser was fit into the structure prior to covering the wing. The wing was reinforced in some areas outside of the scope of the glider kit as the forces acting on the wing are not the same as if it was used as a glider wing. The reinforcements were also made at the clew (aft bottom) part of the wing where the wing connects to the main sheet and also along the area where the mast goes into the wing and through the structure. Reinforcements were made using a harder wood than balsa wood for extra strength. For the covering, standard wing covering (heat shrink wrap) was used. A covering iron was used to seal, shrink and stretch the covering for a smooth finish. When the wing sail was complete, the sail area measured to be approximately 550 in². While this is less than the traditional sail, the size of the glider kit used did not allow for a larger sail area to be constructed. Due to the shape of the wing, one side being flat and the

other side having the wing curvature, the wing sail will perform better on one tack than the other. On starboard tack, where the wind is coming over the starboard or right side of the boat first, the wing sail has the flat side on the bottom side of the flow direction. The wing should perform better on starboard tack (wind coming over the right side of the boat first) than on port tack (wind coming over the left side of the boat first).



Figure 13: Wing sail (left) and traditional sail (right) used for the testing

The test runs were performed at Spreckles Lake in San Francisco, CA. This site was chosen for many reasons. The wind during the time of year for testing (March-April 2015) is very consistent, approximately 5-8 knots in the morning building to 8-10 knots in the afternoon. Also, the water is very flat due to the fact that the lake is small and very shallow, causing little wind chop (waves due to wind) to form. The lake was also an ideal choice because if there was an issue with the boat, it could easily be recovered by either waiting for it to come to shore or using another boat to retrieve the RC Laser. Spreckles Lake also has some fixed buoys in the lake that can be used as the start and ending points of the test run, normalizing the distance covered for each testing run. To measure the distance covered for each test, a laser range finder was used.

During the testing, the following variables were measured for analysis. The date and time of the test run, the sail used, the wind speed, the distance covered, the time to complete the run, the average speed (calculated from the time and distance of the run), and any visual observations of the test run that could

alter the results of the run. Items that have the potential to alter the test run include a sudden gust or lull in the wind, a wave caused by another craft, a wind shift, etc. All of the data for the tests were recorded to an Excel spreadsheet which allows for easy comparison of the data analytically and graphically. Any data that was altered for one of the reasons listed above was thrown out of the analysis.



Figure 14: Testing on Spreckles Lake, traditional sail (left) and wing sail (right)

To get the wind speed, an Anemometer was used and the data recorded. To measure the speed of the boat, a GPS enabled tracker was procured and installed on the boat. The data from the GPS tracker is stored aboard the unit and downloaded later to a computer. The GPS tracker is able to give us the maximum speed for each test run. For the average speed of each test run, a standard stop watch was used to time the run of the boat over the given distance. With the distance of each test run known and controlled, the time of each run gives us the average speed of each run.

To help normalize the testing runs between port tack (wind coming over the left side of the boat first) and starboard tack (wind coming over the right side of the boat first), an appropriate sailing angle needed to be chosen. Sailboats cannot sail directly into the wind because there would not be any pressure difference over the sides of the sail and it would flap or luff in the wind. The area where sailboats cannot sail is shown in the red cross section in figure 15. This is known as the sailing compass rose.

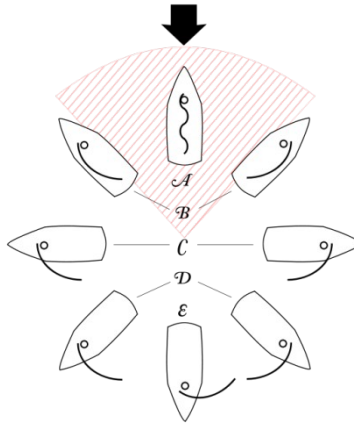


Figure 15: Compass rose of sailing relative to the wind ^G

Per any given wind direction, the points of sail are shown as A, B, C, D, and E which are into the wind, close hauled, beam reach, broad reach, and downwind, respectively. For this experiment, a beam reach of 90 degrees true wind angle was chosen as this is the fastest point of sail typically due to a minimum amount of drag on the sail.

9 Results of Practical Experiment

Testing for the experiment was conducted over a two day period (April 3-4, 2015) at Spreckles Lake as noted above. The conditions were excellent for testing with light winds in the morning on day 1 and slightly stronger breezes on day 2 in the afternoon. Due to the different wind directions seen throughout the testing periods, different distances of test runs were used. For most test runs, a distance between two buoys on the water was used that was 63 feet. When the breeze was further south, the buoy distance per run was increased in order to keep the runs at 90 degree angles to the true wind direction. Even though the true wind angle to the hull was 90 degrees, the true wind angle to the sail (wing or traditional) was kept at about 15 degrees by trimming the sail servo on the boat as it sailed along. The data was entered into the spreadsheet shown in Appendix C. For each testing run, the following items were entered into the spreadsheet, date, time of the test, the sail used, the wind speed during the test, the wind direction, the boat tack, the distance covered and the time it took the boat to cover that distance. From this, the average speed for each run was derived as well as a normalized average speed. The reason for the normalization

is due to the sail area difference between the traditional sail and the wing sail. The normalization factor is 1.3 which is the ratio of the sail area difference between the two sails.

The data was then organized into a graph with each test represented as a data point. The data sets were grouped per sail type and direction (starboard tack traditional sail, port tack traditional sail, starboard tack wing sail and port tack wing sail) and plotted with the wind speed of the test on the x axis and the average speed of the run on the y axis. For each data set, a linear trend line was added to each data set to show the projected average speed per given wind strength. Figure 16 shows all of the test runs on one chart with the linear trend lines for each data set.

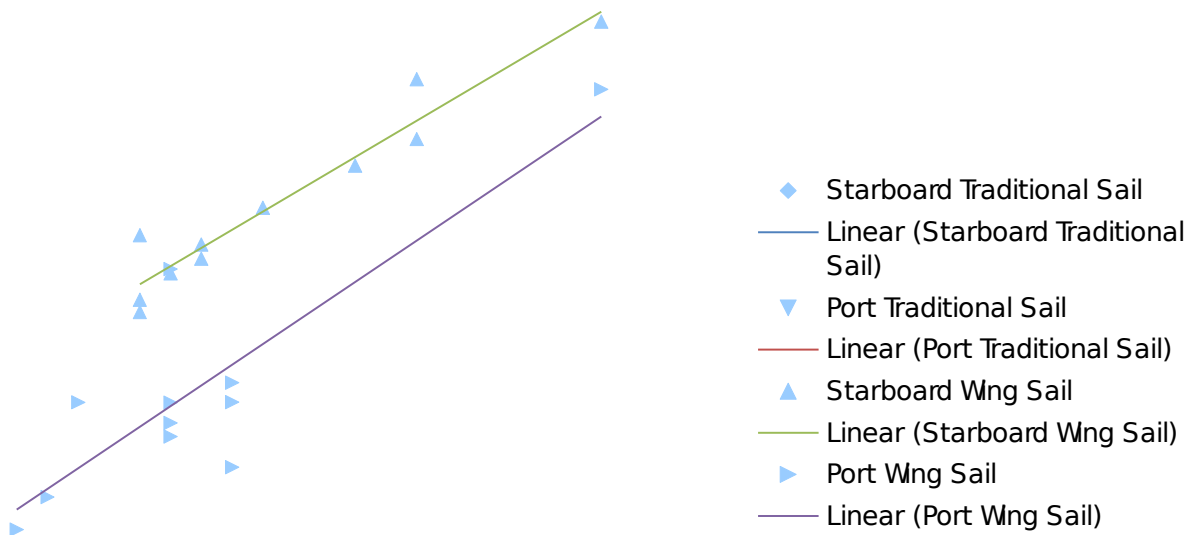


Figure 16: Testing data from experimental tests

Figure 17 shows the normalization of the wing sail data on starboard tack along with the data for the traditional sail and wing sail on starboard tack for the testing period. The figure also includes linear trend lines for the different data sets. For this figure, the port tack testing runs for both sets of sails were omitted.

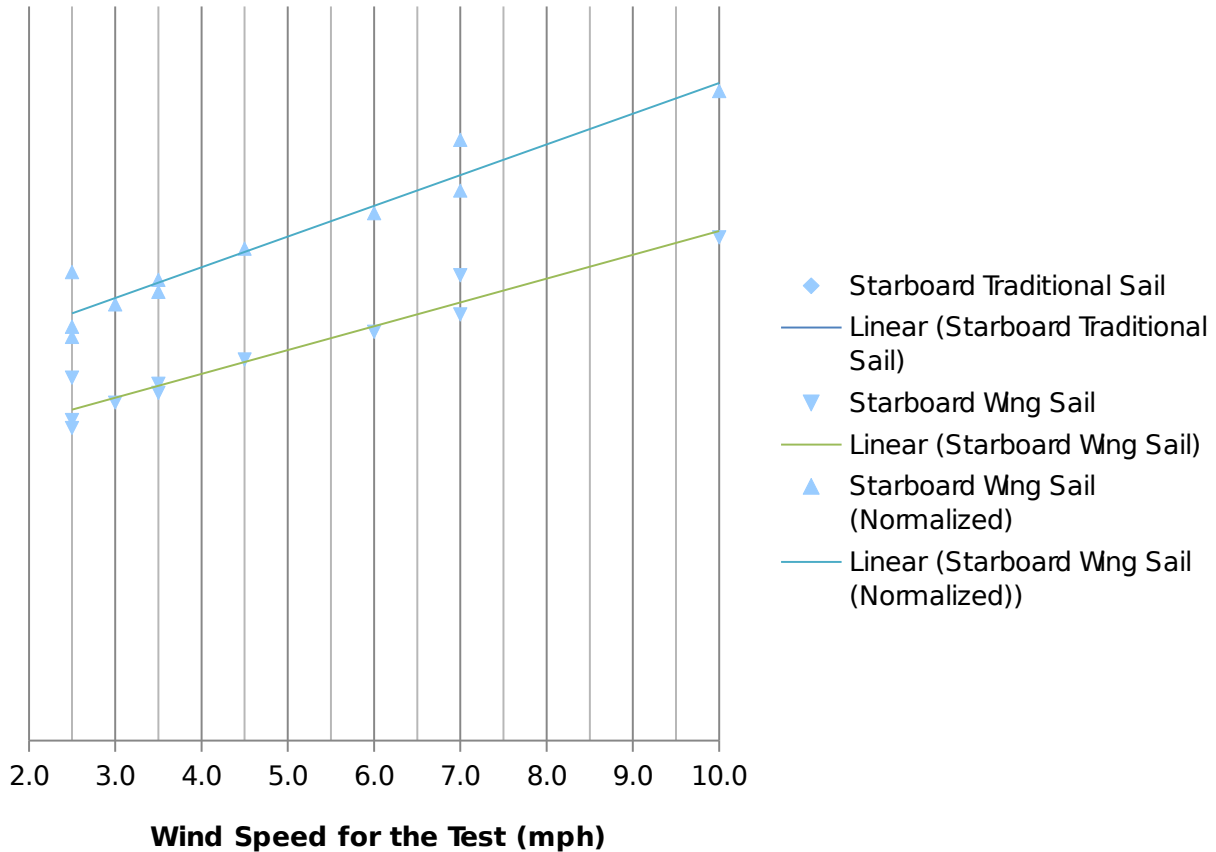


Figure 17: Testing data from experimental tests with normalization of the wing sail data on starboard

10 Discussion of Practical Experimental Analysis

As shown in Figure 16, the results of the testing show that the wing sail was significantly slower on port tack than on starboard tack. This was expected as the wing was not built symmetrical and had a flat side on the starboard side of the wing. When the boat was on starboard tack, the air flow around the wing was similar to what an airplane wing would see and also the theoretical examples. On port tack, the wing was effectively upside-down in relation to the theoretical examples and did not generate nearly as much lift

while producing more drag. The traditional sail has the ability to conform itself to the shape similar to the theoretical example on each tack and as shown it had very similar results on starboard tack as it did on port tack.

When comparing the traditional sail to the wing sail, we can exclude both the port tack wing sail and the port tack traditional sail. This is because the port tack wing sail numbers are not viable (as noted above) and we can get a more direct comparison between sails by using the same tack to eliminate any difference between the two tacks during testing. Figure 17 shows the comparison between the starboard traditional sail (dark blue) and the starboard wing sail (green) test runs. It is worth noting that these results are very similar and have similar trend lines. This shows that the wing sail performance was similar to the traditional sail for this testing.

Keeping in mind that the wing sail had a smaller sail area than the traditional sail (550 in² to 710 in² and shown clearly in Figure 13, a normalization factor was created to further analyze the data. The starboard wing sail data was multiplied by this factor (~1.3) and plotted in Figure 17 as the light blue data set. As you can see, if the wing sail had a similar sail area to the traditional sail, the performance would have been much better and surpassed the performance of the traditional sail.

5. General Discussion

Through a theoretical analysis using a CFD modeling software package and a practical experiment it has been shown that a wing sail can perform at minimum similar and most of the time better than a traditional sail on a small sailing craft at low speeds. This is mostly due to the flow around the wing section being far more uniform than that around the traditional sail. This allows the drag of the wing sail to be lower while also producing the same amount or more lift and thus a higher lift to drag ratio for the section. This was true at many different wind speeds and also at different angles of attack.

Even with the simple, smaller wing section chosen for the practical experiment, the results between the wing sail and traditional sail were almost identical. If the wing sail was more efficient and also the same size as the traditional sail, the wing sail could have outperformed the traditional sail as shown by the normalized data in Figure 17. The wing sail also suffered from inefficiency on port tack due to the shape of the wing. Modern wing sail designs have gotten past that by developing wings that have two sections that camber between them to form an airfoil that is the same on both tacks. Each section of the wing is symmetrical in itself but the two sections are angled relative to each other to form the air foil. An example of how the cambered wing sail would look can be seen in Figure 18.

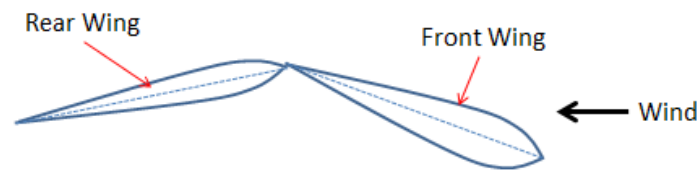


Figure 18: Two section camber wing cross-section

Another way that the wing sail could be more efficient is to build up apparent wind. As the boat speed begins to build, the amount of apparent wind around the sail grows and the angle of attack gets smaller. The traditional sail would hit a limit point where the angle of attack would be too shallow and the amount of lift developed would not overcome the amount of drag being developed. Since the wing sail has a more efficient shape, the amount of lift developing would be higher than the amount of drag being developed and you would have potential for exponential growth for the amount of apparent wind as the angle of attack gets smaller.

For the 33rd America's Cup, Oracle Team USA, the defenders and eventual winner used a winged main sail for their boat. The wing sail was two sections and would camber between the two sections to provide the angle of attack on each port tack and starboard tack. The wing sail was so efficient that the boat was able to sail at speeds of over 46 mph in only 20 mph of wind. The boat speeds downwind were

particularly impressive as the boat's apparent wind angle built up to a level where the wing was trimmed similar to how one would trim it going upwind.



Figure 19: Oracle Team USA, winner of the 34th America's Cup with their cambered wing main sail ⁴

Further experimentation should take place with the wing sail and the traditional sail at higher wind speeds to find out if there is a limit to the performance of the wing sail. Judging by how sailing speed records continue to be broken by craft with wing sails versus traditional sails, it is plausible to believe that the wing sail will continue to perform similar if not better than the traditional sail at higher wind speeds. Follow on testing could also be performed with cambered wing sections that allow the sailboat to perform equally better on both port and starboard tack as well. The build for this setup would be more complex and might require a testing platform that has more servo control than the one used for this experiment.

Further theoretical testing can also be performed at different angles of attack in order to find the optimum angle of attack for both the traditional sail and the wing sail for different wind speeds. This data could be useful in development of larger applications of both types of sails.

6. Conclusions

For small sailboats at lower wind speeds, the wing sail had a similar or greater performance than that of the traditional sail. The theory that has been applied to larger sailboats and wing sections at higher speeds holds true for boats of a smaller scale and can be adapted to modern sailing designs. The facts found in this paper can help to begin to develop larger applications of wing sails to be used on sailboats, commercial vessels, spacecraft, and any other application that uses modern sailing principles. As in previous versions of the America's Cup developing the latest sailing technology, the application of a wing sail outperforming a traditional sail is one that will reverberate through the technical community forever.

References

- ¹Jo, Yeongmin, Lee, Hakjin, and Choi, Seongim, "Aerodynamic Design Optimization of Wing-Sails," Fluid Dynamics and Co-located Conferences, *31st AIAA Applied Aerodynamics Conference*, AIAA 2013-2524, June 2013
- ²Ulbrich, Norbert, "Australia II or Secrets of the Upside-Down Winged Keel Design", *41st Aerospace Sciences Meeting and Exhibit*, AIAA 2003-39, January 2003
- ³Rosen, Bruce S., Laiosa, Joseph P., Davis Jr., Warren H., "CFD Design Studies for America's Cup 2000", AIAA-2000-4339
- ⁴Engblom, W.A., "Development of an Atmospheric Satellite Concept Based on Sailing", *52nd Aerospace Sciences Meeting*, AIAA 2014-1111, January 2014
- ⁵Wilkins, Matthew P., Subbarao, Kamesh, Alfriend, Kyle T., Vadali, Srinivas R., "Modeling and Simulation of a Power Sail", *AIAA/AAS Astrodynamics Specialist Conference and Exhibit*, AIAA 2002-4519, August 2002
- ⁶Jameson, Antony, Jameson, Sriram, and Gerritsen, Margot G., "Numerical Analysis and Design of Upwind Sails", *21st Applied Aerodynamics Conference*, AIAA 2003-3501, June 2003
- ⁷Junge, Timm, Gerhardt, Frederik C., Richards, Peter, and Flay, Richard G.J., "Optimizing Spanwise Lift Distributions Yacht Sails Using Extended Lifting Line Analysis", *Journal of Aircraft*, Vol. 47, No. 6, November-December 2010
- ⁸Guthrie, Julian, *The Billionaire and the Mechanic*, Grove Press, Reprint Edition, 2014
- ⁹Swintal, Diane, Tsuchiya, R. Steven, Kamins, Robert, *Winging It: ORACLE TEAM USA's Incredible Comeback to Defend the America's Cup*, International Marine/Ragged Mountain Press, December 2013
- ¹⁰Bethwaite, Frank, *High Performance Sailing*, McGraw-Hill Companies, Reprint 2001 Edition
- ¹¹Pulliam, T.H., "Solution Methods in Computational Fluid Dynamics", NASA Ames Research Center, MS T27B-1, January 1986
- ¹²Gomes, L.D. and Kontis, K., "Mast Device for Aerodynamic Improvement of Sail Boats", *2nd AIAA Flow Control Conference*, AIAA 2004-2320, July 2004
- ¹³Curtiss Jr., H.C., "Upright Sailing Craft Performance and Optimum Speed to Windward", *Journal Hydronautics* Vol. 11, No.2

Figure Sources

^AFigure 1: The 1988 America's Cup Match, NZ (far) vs USA (near),
<http://www2.worldpub.net/images/sw/124-FBWarRosesSt.jpg>

^BFigure 2: USA 17 with its traditional soft sail,
http://upload.wikimedia.org/wikipedia/commons/a/a4/BMW_Oracle_BOR90.JPG ,

^CFigure 2: USA 17 with the wing mast and sail,
<http://upload.wikimedia.org/wikipedia/commons/thumb/0/0f/USA-17-flying-cropped.jpg/275px-USA-17-flying-cropped.jpg>

^DFigure 2: USA 17 and Alinghi 5 racing in the 2010 America's Cup,
<http://threesheetsnw.com/files/2010/12/AmericasCup2010.jpg>

^EFigure 3: Vestas Sail Rocket on its record run, http://www.one.sail-world.com/photos_2012_3/Alt_run%20222324%2030.11.2011%20051.jpg

^FFigure 5: Flow over an air foil,
<http://upload.wikimedia.org/wikipedia/en/6/66/NASANewtons3rdGlennResearchCenter.gif>

^GFigure 11: Compass rose of sailing relative to the wind
http://upload.wikimedia.org/wikipedia/commons/thumb/4/4b/Points_of_sail.svg/640px-Points_of_sail.svg.png

^HFigure 19: Oracle Team USA, winner of the 33rd America's Cup with their cambered wing main sail,
<http://www.cupinfo.com/images/or-72-speed-ggotu-6782-1.jpg>

Appendix A: Grid Patterns for the Theoretical Mesh Models

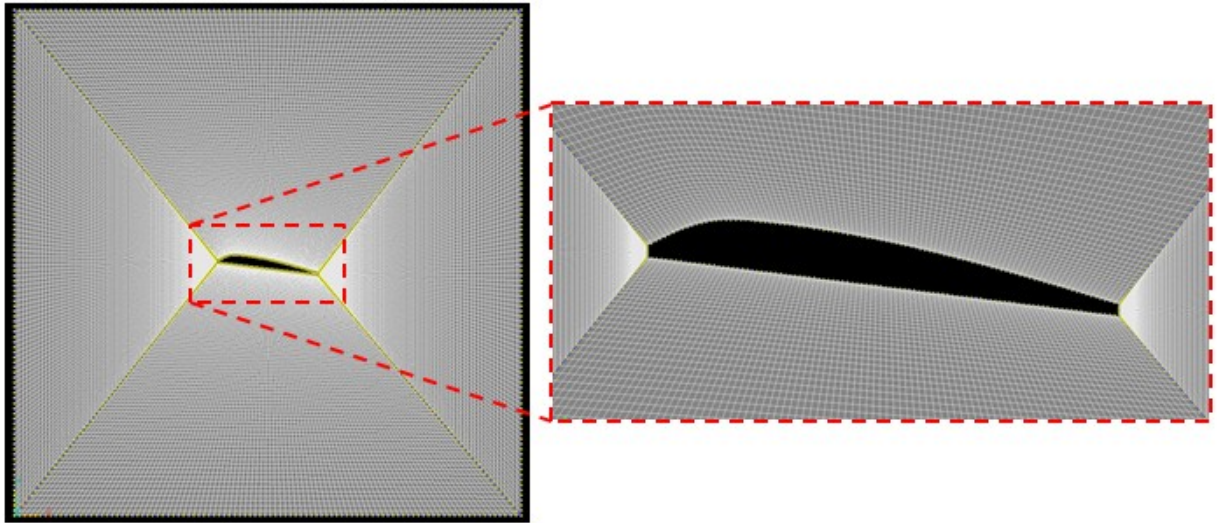


Figure 20: Grid mesh for wing sail section with 14 degrees angle of attack

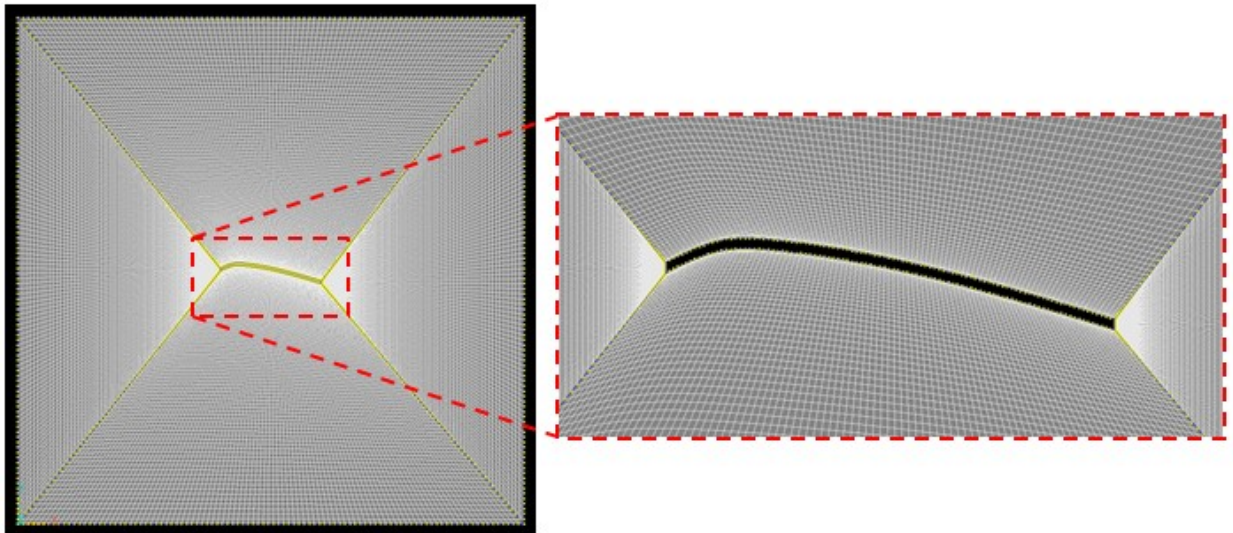


Figure 21: Grid mesh for traditional sail section with 14 degrees angle of attack

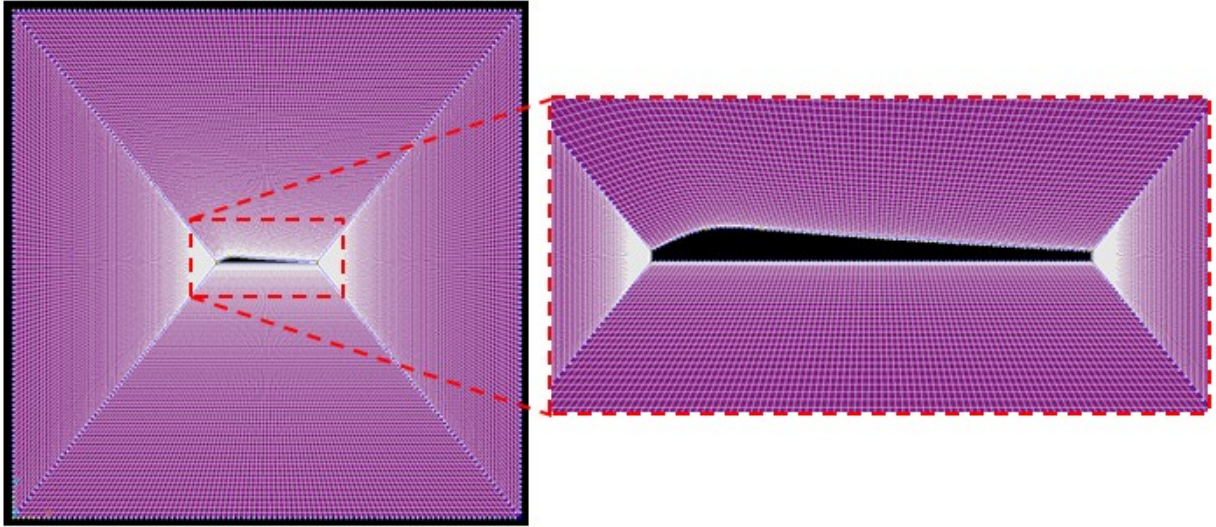


Figure 22: Grid mesh for wing sail section with 0 degrees angle of attack

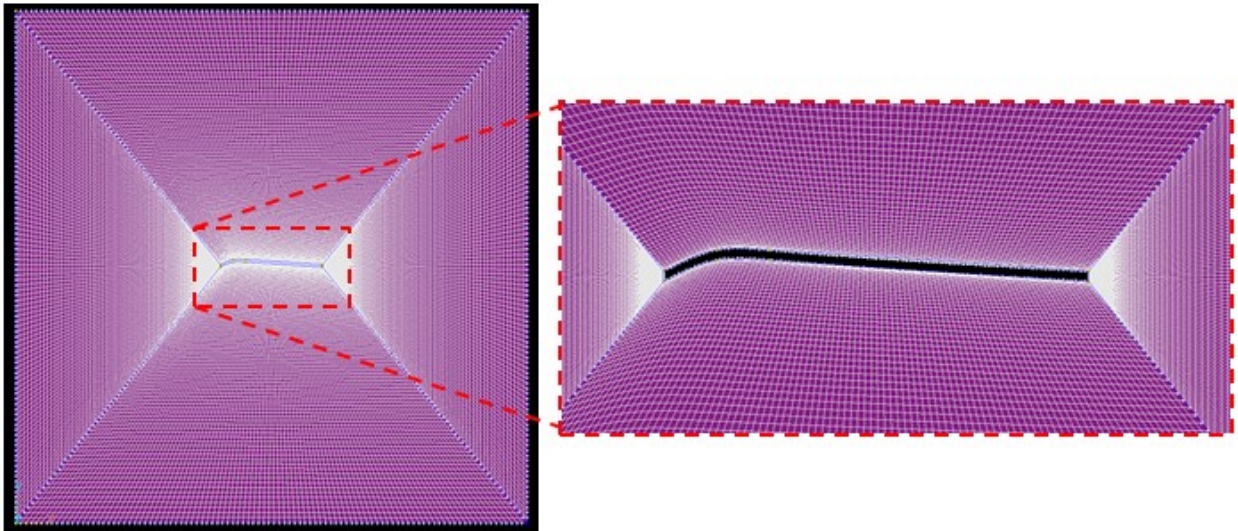


Figure 23: Grid mesh for traditional sail section with 0 degrees angle of attack

Appendix B: Theoretical Experiment Results

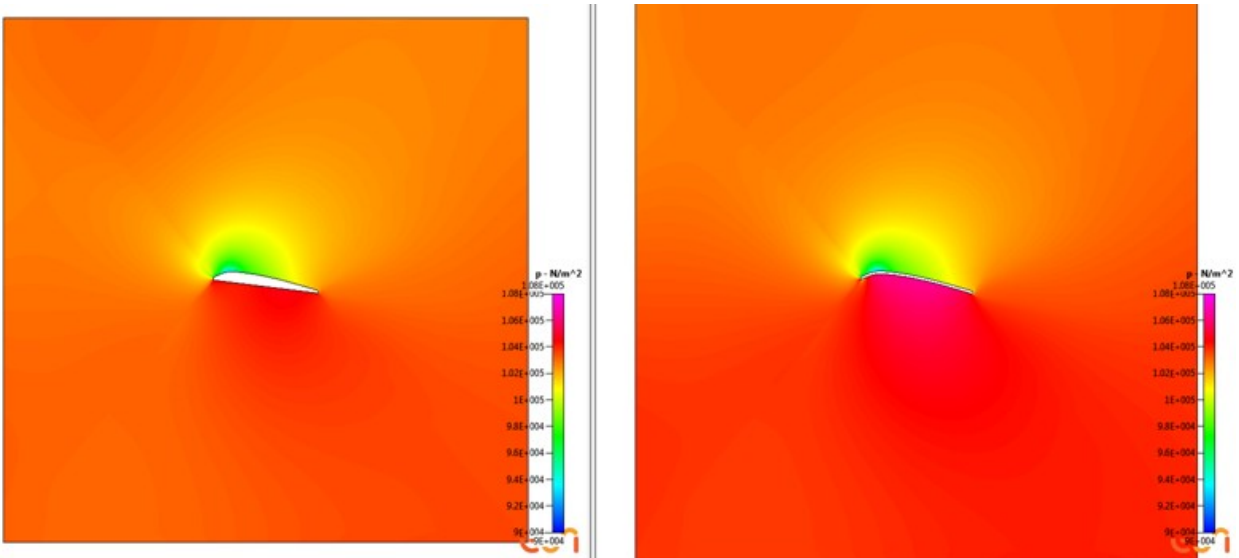


Figure 24: Pressure distribution at 14° angle of attack and 100 m/s for a wing (left) and a traditional sail (right)

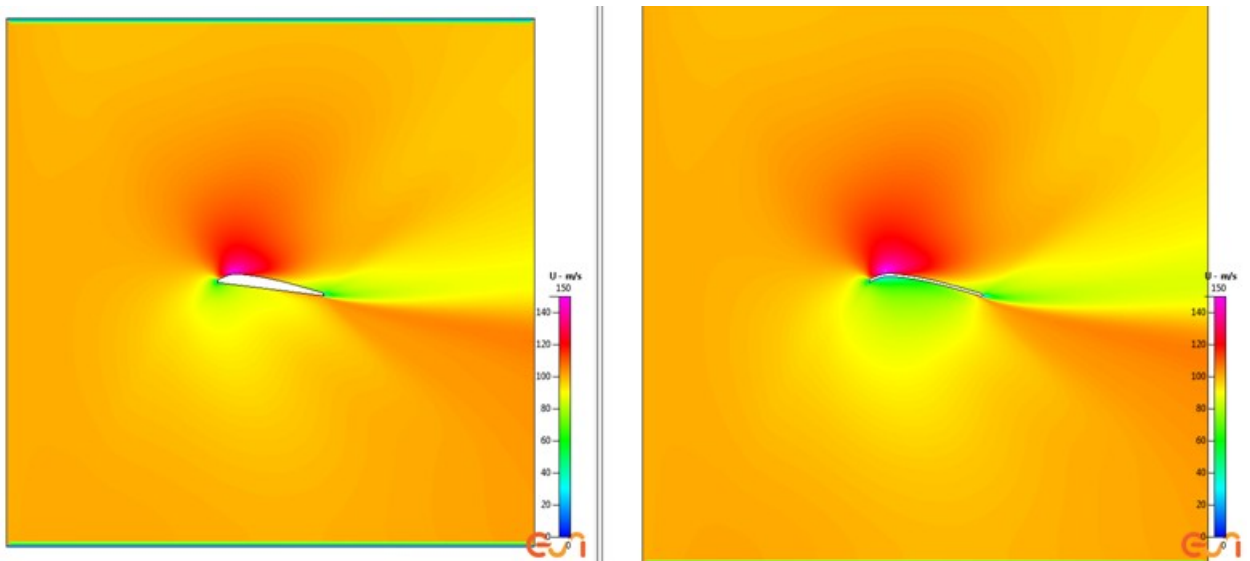


Figure 25: Flow Velocity at 14° angle of attack and 100 m/s for a wing (left) and a traditional sail (right)

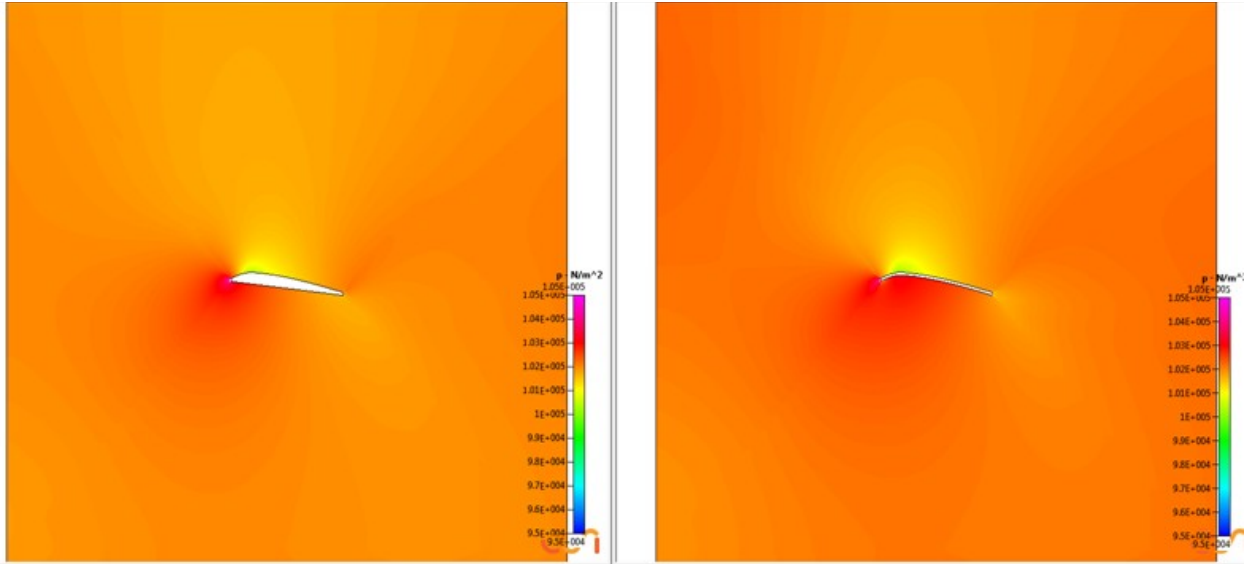


Figure 26: Pressure distribution at 14° angle of attack and 50 m/s for a wing (left) and a traditional sail (right)

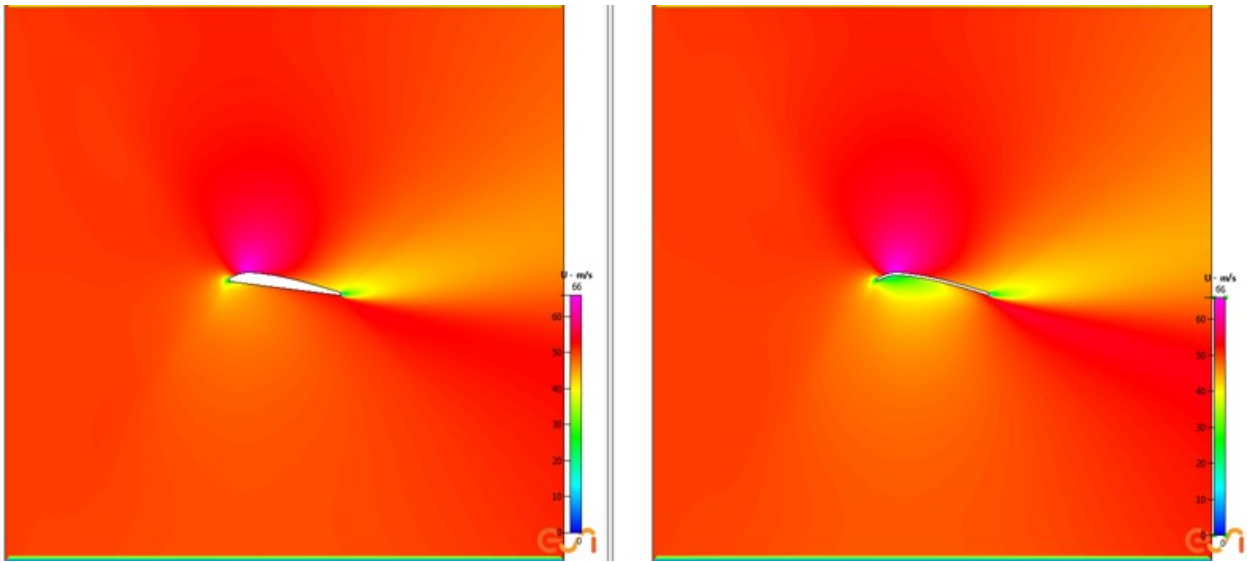


Figure 27: Flow Velocity at 14° angle of attack and 50 m/s for a wing (left) and a traditional sail (right)

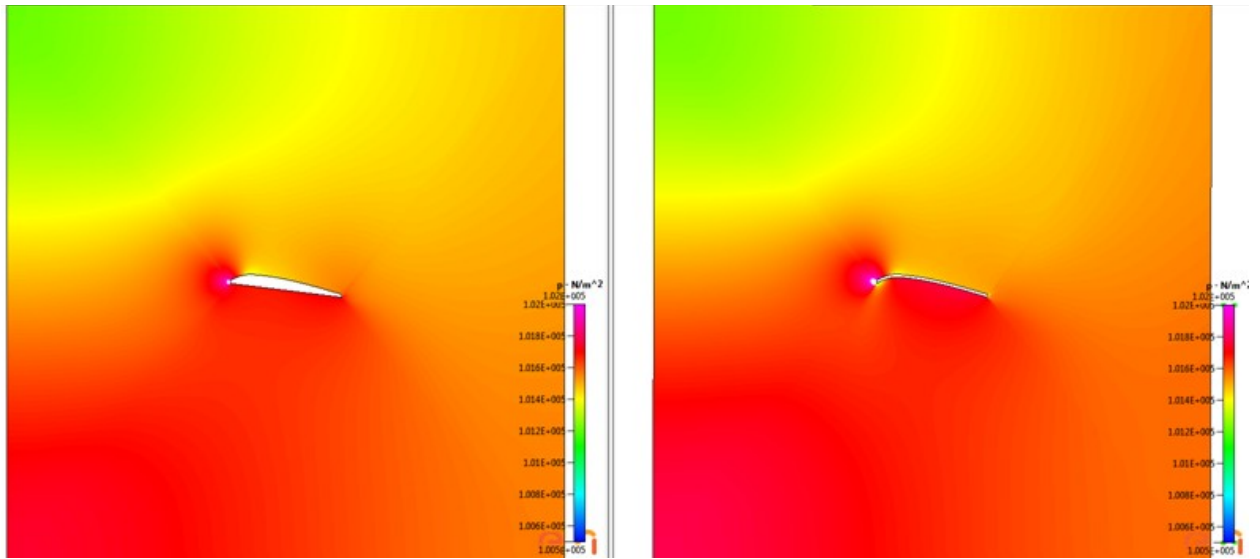


Figure 28: Pressure distribution at 14° angle of attack and 20 m/s for a wing (left) and a traditional sail (right)

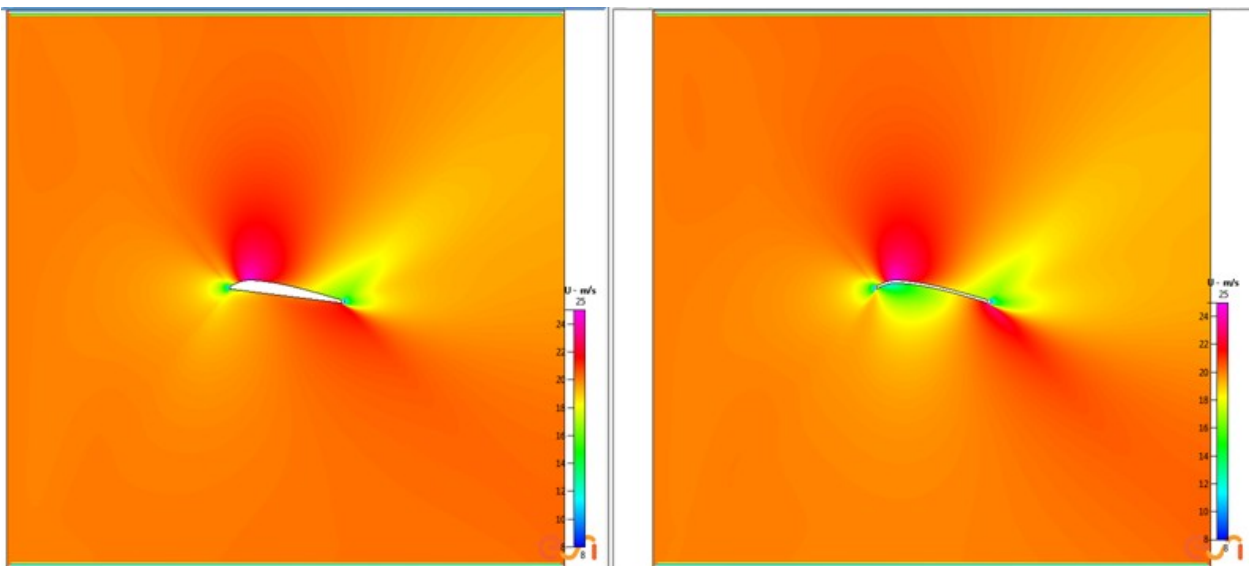


Figure 29: Flow Velocity at 14° angle of attack and 20 m/s for a wing (left) and a traditional sail (right)

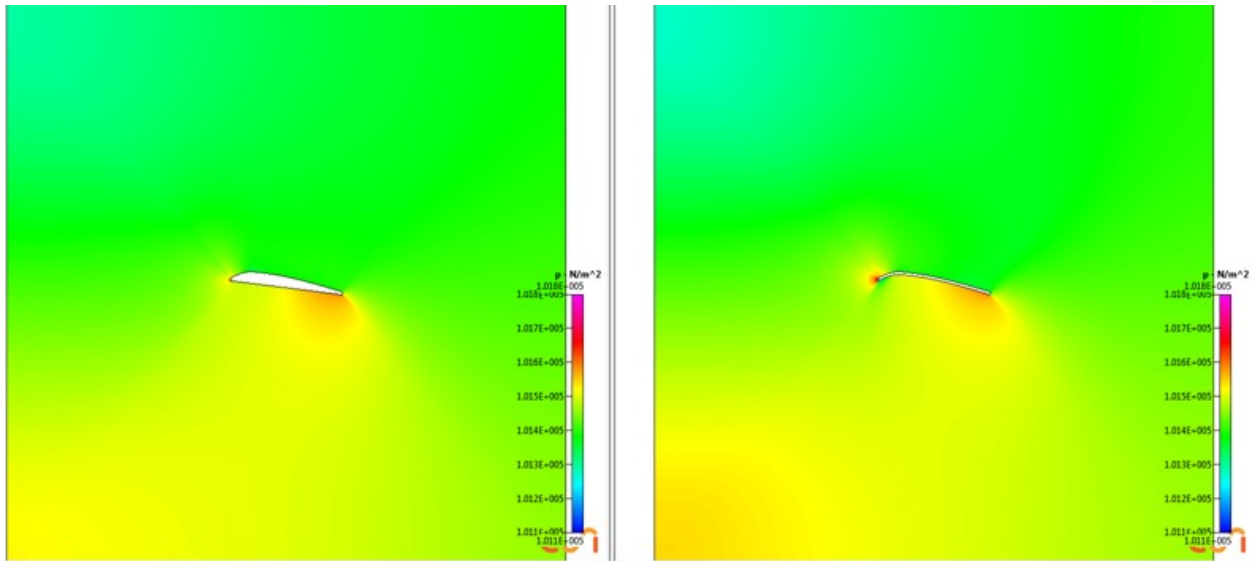


Figure 30: Pressure distribution at 14° angle of attack and 10 m/s for a wing (left) and a traditional sail (right)

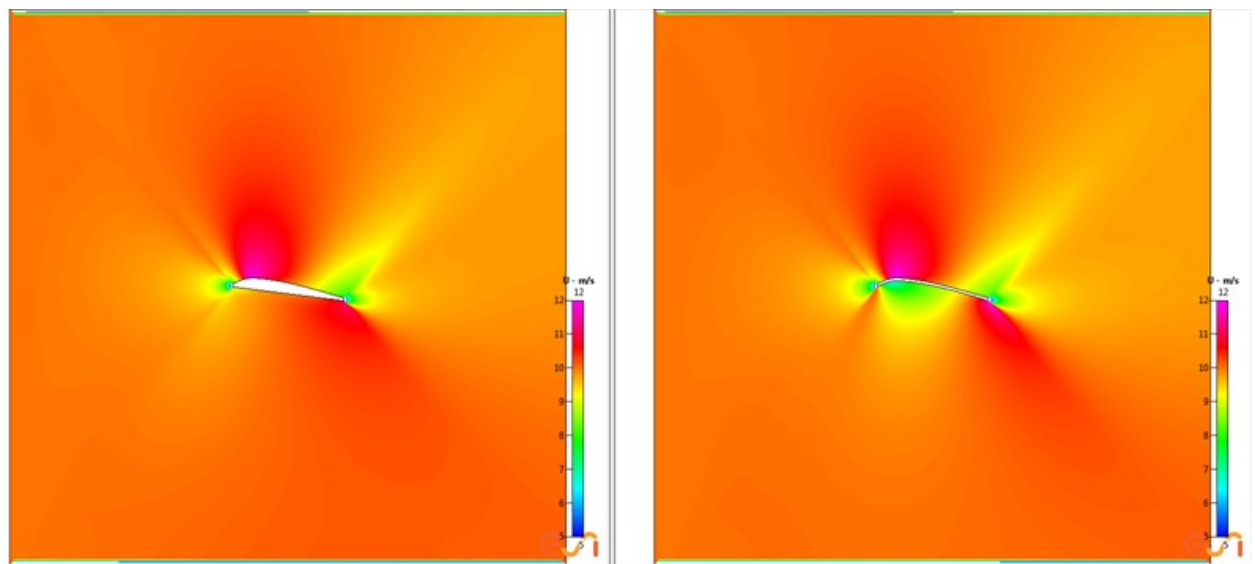


Figure 31: Flow Velocity at 14° angle of attack and 10 m/s for a wing (left) and a traditional sail (right)

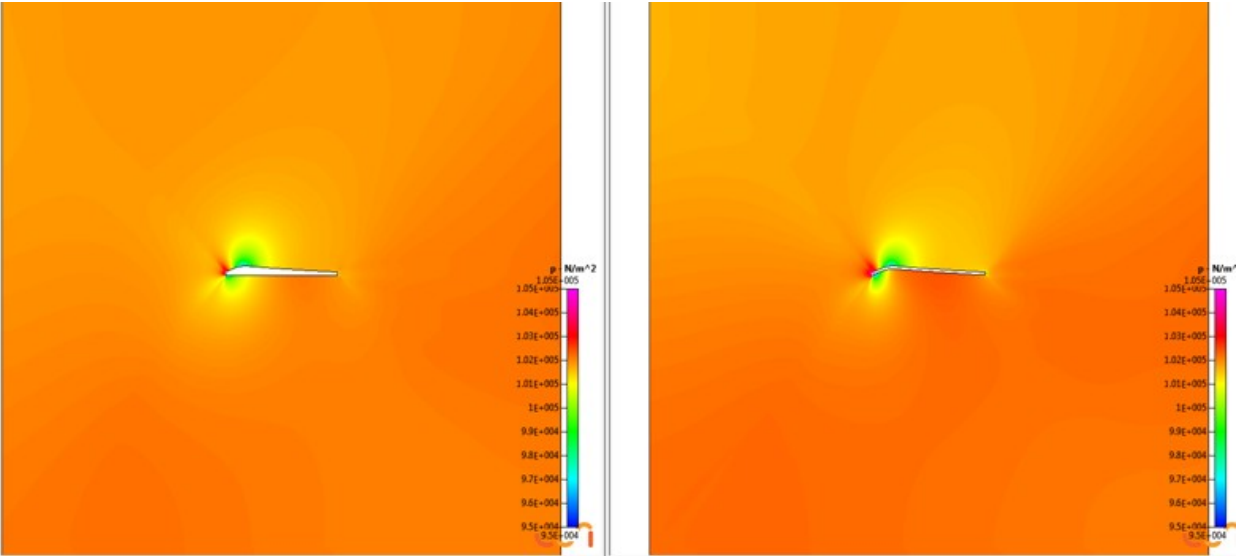


Figure 32: Pressure distribution at 0° angle of attack and 100 m/s for a wing (left) and a traditional sail (right)

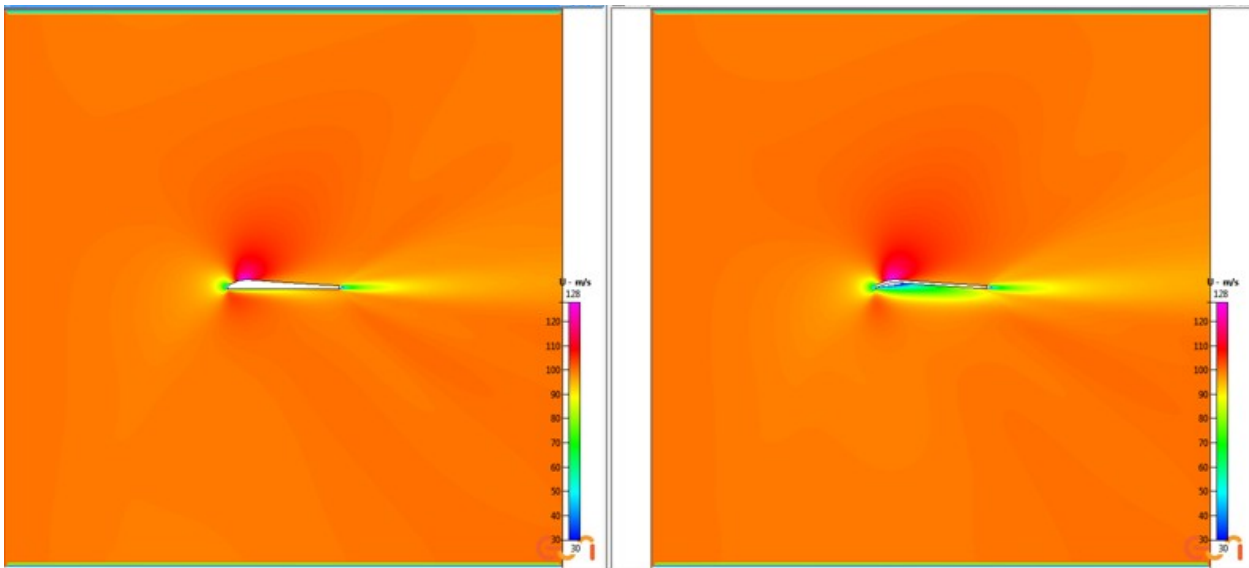


Figure 33: Flow Velocity at 0° angle of attack and 100 m/s for a wing (left) and a traditional sail (right)

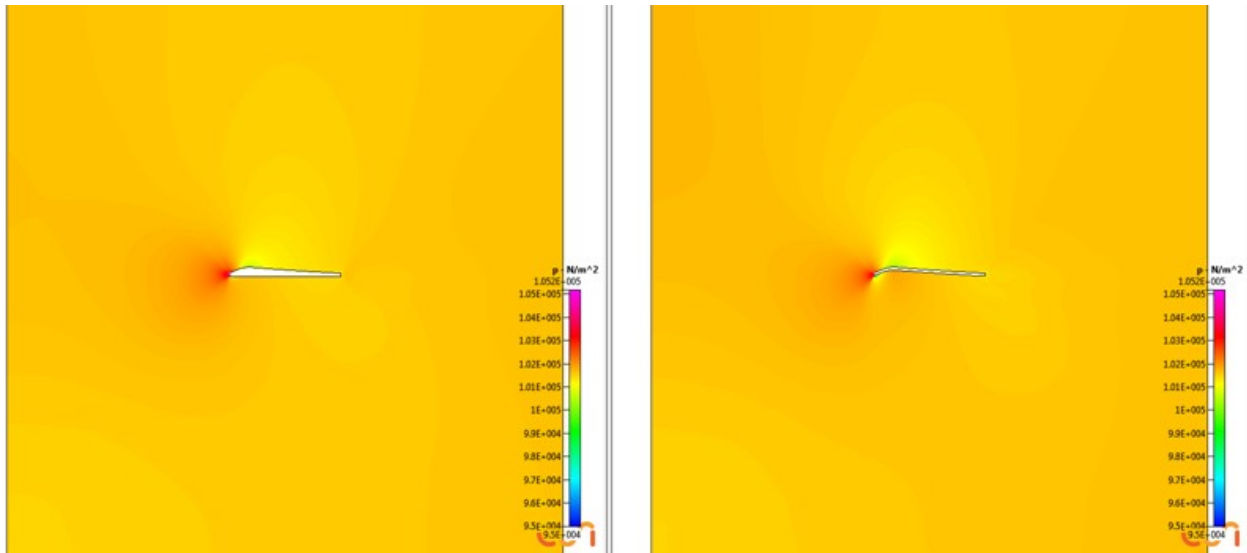


Figure 34: Pressure distribution at 0° angle of attack and 50 m/s for a wing (left) and a traditional sail (right)

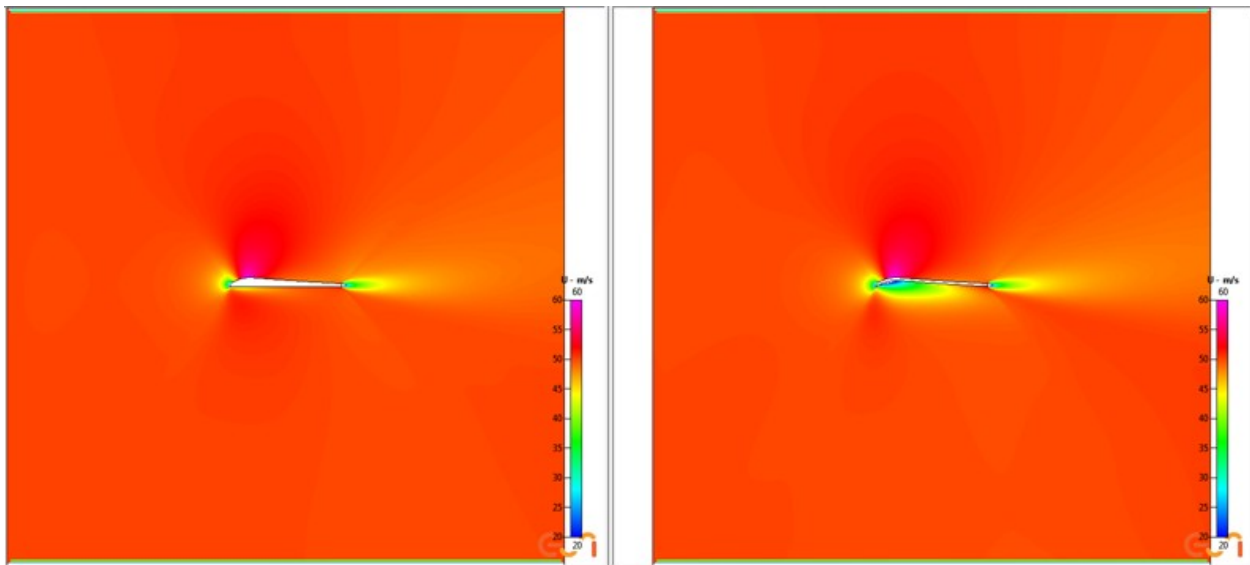


Figure 35: Flow Velocity at 0° angle of attack and 50 m/s for a wing (left) and a traditional sail (right)

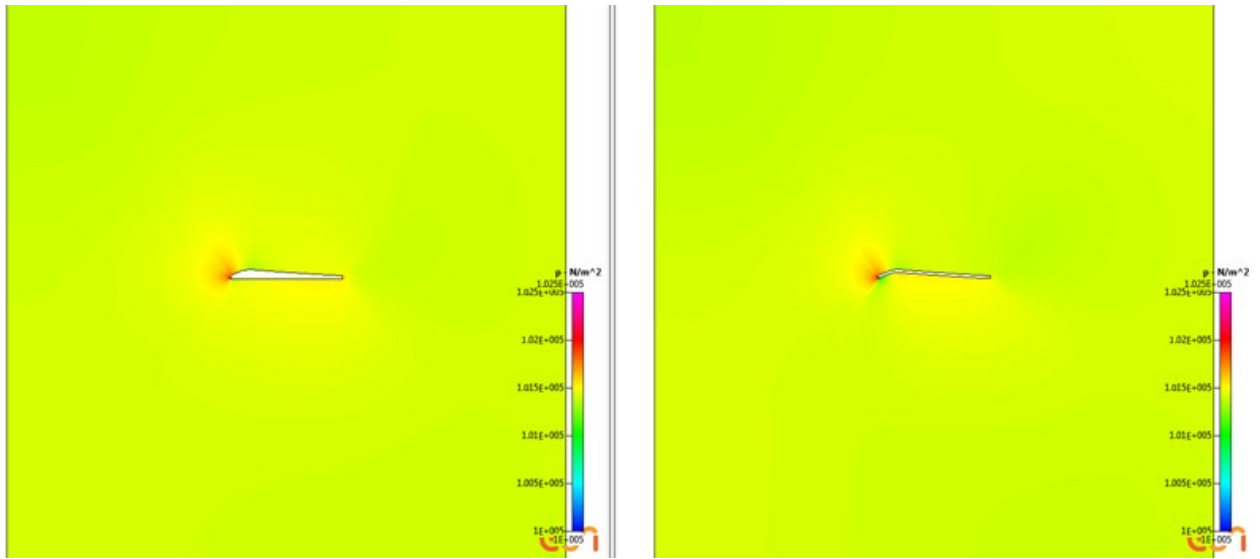


Figure 36: Pressure distribution at 0° angle of attack and 20 m/s for a wing (left) and a traditional sail (right)

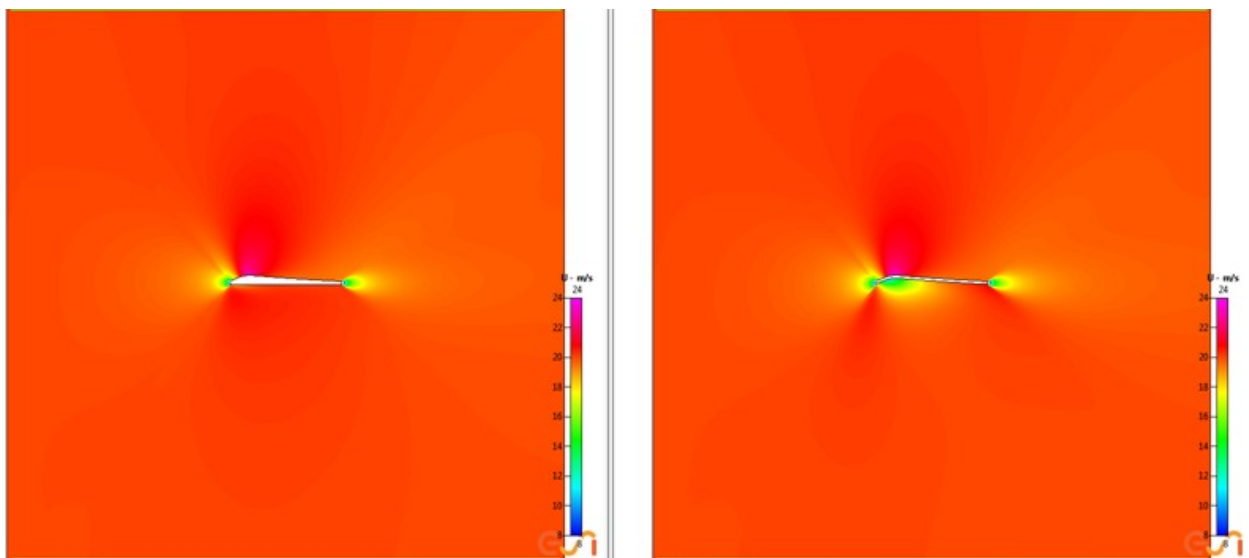


Figure 37: Flow Velocity at 0° angle of attack and 20 m/s for a wing (left) and a traditional sail (right)

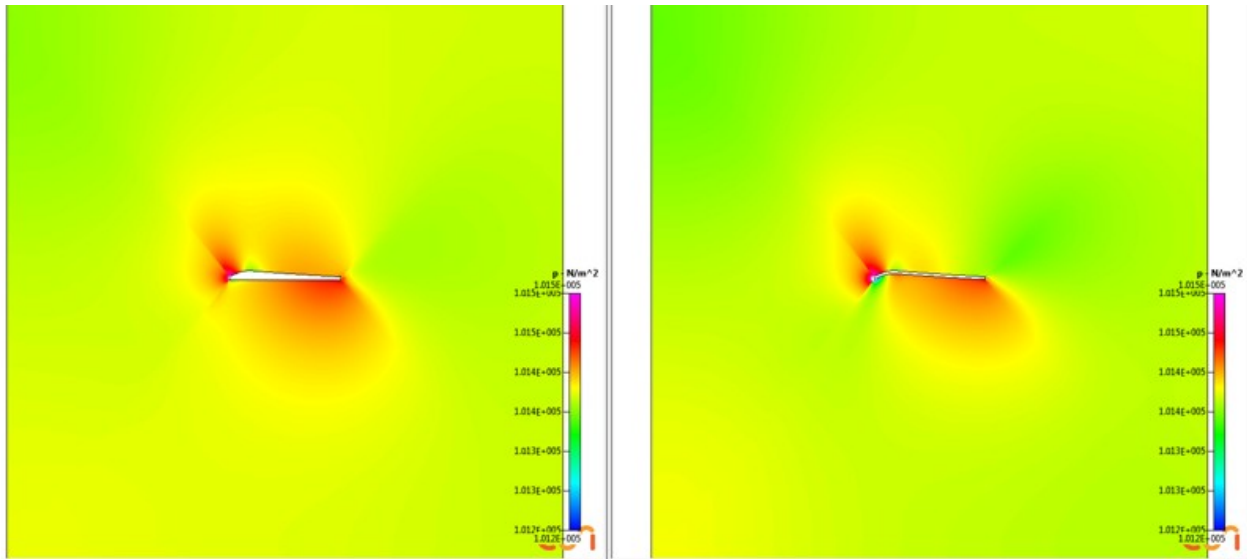


Figure 38: Pressure distribution at 0° angle of attack and 10 m/s for a wing (left) and a traditional sail (right)

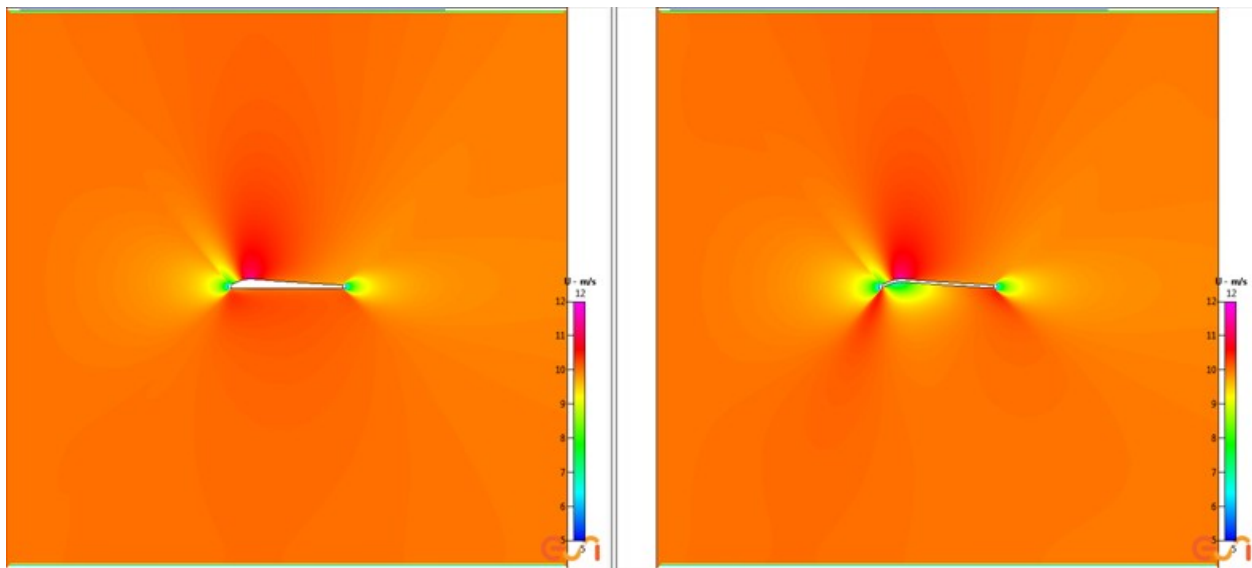


Figure 39: Flow Velocity at 0° angle of attack and 10 m/s for a wing (left) and a traditional sail (right)

Appendix C: Practical Experiment Raw Testing Data

Table 2: Practical experiment testing data

Location: Spreckles Lake in San Francisco, CA

| Date | Time | Sail Used | Wind Speed (mph) | Wind Dir. | Boat Tack | Distance (ft) | Time (sec) | Avg Speed (mph) | Normalized (mph) |
|----------|-------|-------------|------------------|-----------|-----------|---------------|------------|-----------------|------------------|
| 04/03/15 | 11:01 | Traditional | 2.0 | SW | Starboard | 108 | 41.92 | 1.76 | 1.76 |
| 04/03/15 | 11:05 | Traditional | 1.5 | SW | Starboard | 108 | 48.49 | 1.52 | 1.52 |
| 04/03/15 | 11:11 | Traditional | 1.5 | S | Starboard | 120 | 32.24 | 2.54 | 2.54 |
| 04/03/15 | 11:15 | Traditional | 1.5 | S | Starboard | 120 | 40.95 | 2.00 | 2.00 |
| 04/03/15 | 11:36 | Traditional | 5.0 | SW | Starboard | 63 | 17.79 | 2.41 | 2.41 |
| 04/03/15 | 11:38 | Traditional | 4.0 | SW | Starboard | 63 | 23.89 | 1.80 | 1.80 |
| 04/03/15 | 11:40 | Traditional | 3.0 | SW | Starboard | 63 | 23.51 | 1.83 | 1.83 |
| 04/04/15 | 15:54 | Traditional | 6.0 | SW | Starboard | 63 | 17.76 | 2.42 | 2.42 |
| 04/04/15 | 16:00 | Traditional | 9.0 | SW | Starboard | 63 | 12.85 | 3.34 | 3.34 |
| 04/04/15 | 16:02 | Traditional | 6.0 | SW | Starboard | 63 | 17.00 | 2.53 | 2.53 |
| 04/03/15 | 11:03 | Traditional | 3.5 | SW | Port | 108 | 24.92 | 2.95 | 2.95 |
| 04/03/15 | 11:09 | Traditional | 3.0 | S | Port | 108 | 49.94 | 1.47 | 1.47 |
| 04/03/15 | 11:13 | Traditional | 1.0 | S | Port | 120 | 54.86 | 1.49 | 1.49 |
| 04/03/15 | 11:37 | Traditional | 1.5 | SW | Port | 63 | 23.66 | 1.82 | 1.82 |
| 04/03/15 | 11:39 | Traditional | 3.5 | SW | Port | 63 | 23.81 | 1.80 | 1.80 |
| 04/03/15 | 11:41 | Traditional | 2.5 | SW | Port | 63 | 26.43 | 1.63 | 1.63 |
| 04/04/15 | 15:57 | Traditional | 6.0 | SW | Port | 63 | 17.61 | 2.44 | 2.44 |
| 04/04/15 | 16:00 | Traditional | 7.0 | SW | Port | 63 | 16.86 | 2.55 | 2.55 |
| 04/04/15 | 16:08 | Traditional | 7.0 | SW | Port | 63 | 16.91 | 2.54 | 2.54 |
| 04/03/15 | 11:26 | WingSail | 3.0 | S | Starboard | 63 | 20.74 | 2.07 | 2.67 |
| 04/03/15 | 11:28 | WingSail | 3.5 | SW | Starboard | 63 | 20.16 | 2.13 | 2.75 |
| 04/03/15 | 11:30 | WingSail | 4.5 | SW | Starboard | 63 | 18.39 | 2.34 | 3.02 |
| 04/03/15 | 11:32 | WingSail | 2.5 | SW | Starboard | 63 | 22.42 | 1.92 | 2.47 |
| 04/03/15 | 11:43 | WingSail | 3.5 | SW | Starboard | 63 | 19.64 | 2.19 | 2.82 |
| 04/03/15 | 11:45 | WingSail | 2.5 | SW | Starboard | 63 | 21.86 | 1.96 | 2.54 |
| 04/03/15 | 11:52 | WingSail | 2.5 | SW | Starboard | 63 | 19.31 | 2.22 | 2.87 |
| 04/04/15 | 16:10 | WingSail | 7.0 | SW | Starboard | 63 | 16.45 | 2.61 | 3.37 |
| 04/04/15 | 16:12 | WingSail | 6.0 | SW | Starboard | 63 | 17.15 | 2.50 | 3.23 |
| 04/04/15 | 16:13 | WingSail | 10.0 | SW | Starboard | 63 | 13.93 | 3.08 | 3.98 |
| 04/04/15 | 16:17 | WingSail | 7.0 | SW | Starboard | 63 | 15.06 | 2.85 | 3.68 |
| 04/03/15 | 11:27 | WingSail | 4.0 | SW | Port | 63 | 33.25 | 1.29 | 1.67 |
| 04/03/15 | 11:29 | WingSail | 3.0 | SW | Port | 63 | 30.34 | 1.42 | 1.83 |
| 04/03/15 | 11:31 | WingSail | 3.0 | SW | Port | 63 | 29.21 | 1.47 | 1.90 |
| 04/03/15 | 11:33 | WingSail | 3.0 | SW | Port | 63 | 20.57 | 2.09 | 2.70 |
| 04/03/15 | 11:44 | WingSail | 0.5 | SW | Port | 63 | 41.27 | 1.04 | 1.34 |
| 04/03/15 | 11:46 | WingSail | 1.5 | SW | Port | 63 | 27.66 | 1.55 | 2.00 |
| 04/03/15 | 11:53 | WingSail | 1.0 | SW | Port | 63 | 36.66 | 1.17 | 1.51 |
| 04/04/15 | 16:10 | WingSail | 4.0 | SW | Port | 63 | 26.33 | 1.63 | 2.11 |
| 04/04/15 | 16:12 | WingSail | 10.0 | SW | Port | 63 | 15.28 | 2.81 | 3.63 |
| 04/04/15 | 16:14 | WingSail | 3.0 | SW | Port | 63 | 27.68 | 1.55 | 2.00 |
| 04/04/15 | 16:17 | WingSail | 4.0 | SW | Port | 63 | 27.65 | 1.55 | 2.01 |